6-4-2009

CAREER: Acoustic Wave Filters for High Frequency Wireless Communication Applications

Mauricio Pereira da Cunha
Principal Investigator; University of Maine, Orono, mdacunha@maine.edu

Final Report for Period: 03/2008 - 02/2009 **Submitted on:** 06/04/2009

Principal Investigator: Pereira da Cunha, Mauricio . **Award ID:** 0134335

Organization: University of Maine

Submitted By:

Pereira da Cunha, Mauricio - Principal Investigator

Title:

CAREER: Acoustic Wave Filters for High Frequency Wireless Communication Applications

Project Participants

Senior Personnel

Name: Pereira da Cunha, Mauricio

Worked for more than 160 Hours: Yes

Contribution to Project:

Prof. Pereira da Cunha is the PI on this project and directly responsible for all the activities involved in this initiative.

Name: Beenfeldt, Eric

Worked for more than 160 Hours: No

Contribution to Project:

Eric has been instrumental in advising students, providing support in equipment maintenance, and in the development of measurement techniques.

Name: Hummels, Donald

Worked for more than 160 Hours: No

Contribution to Project:

Prof. Don Hummels was involved in the advising of Jason Withee (NSF REU summer 2007) and Evan Dudzik regarding the implementation of the signal processing acquisition board.

Name: Abedi, Ali

Worked for more than 160 Hours: No

Contribution to Project:

Prof. Abedi was involved in advising Evan Dudzik in the selection of codes for implementation in the spread spectrum wireless passive surface acoustic wave tags. He is supported in part by a NASA/Maine Space Research Consortium research effort.

Post-doc

Graduate Student

Name: Thiele, Jeremy

Worked for more than 160 Hours: No

Contribution to Project:

Jeremy performed his MS on new materials and harsh environment gas sensors with partial support from the NSF Career project (equipment usage, materials). He was mostly funded by a Maine Space Grant Consortium/NASA Funds.

Name: Kenny, Thomas

Worked for more than 160 Hours: Yes

Contribution to Project:

Tom is concluding his PhD thesis in the proposal topic. He has been fully funded by the NSF Career project and worked on the identification of new orientations and device modeling for the new modes identified.

Name: Dudzik, Evan

Worked for more than 160 Hours: Yes

Contribution to Project:

Evan is developing his MS in acoustic wave filter applications for passive wireless surface acoustic wave tags and interrogating

system for about two years. He is supposed to present his thesis in the second semester of 2008. He has been partially funded by the NSF Career and partially by a Maine Space Grant Consortium / NASA funds.

Name: Pollard, Thomas

Worked for more than 160 Hours: Yes

Contribution to Project:

Tom is developing his thesis on Biosensors and is funded by another NSF grant under the Sensors initiative. His involvement in this project relates to the development of methods for device modeling and acoustic wave directions propagation, a topic that has common denominator with the work performed by Thomas Kenny, previously identified.

Name: Davulis, Peter

Worked for more than 160 Hours: Yes

Contribution to Project:

Peter started working on this project as as an NSF REU student in 2005 in the characterization of gallium orthophosphate, a new piezoelectric crystal. Out of his efforts he generated a conference paper in the IEEE 2006 Frequency Control Symposium. After that work, he became a graduate student under my advisory, working on the characterization of LGX crystals in harsh environment. He is being supported mostly by a Petroleum Research Fund grant at this point in time.

Undergraduate Student

Name: Meulendyk, Bennett

Worked for more than 160 Hours: Yes

Contribution to Project:

Bennett worked in this project as a NSF REU student. His work resulted in both conference and journal publications. He is presently a graduate student under my advisory working on another NSF Gas Sensor project in a multidisciplinary team with Chemical Engineering and Spatial Sciences.

Name: Rioux, Benjamin

Worked for more than 160 Hours: No

Contribution to Project:

Ben worked on this project in the 2003 timeframe on the extraction of dielectric constants of piezoelectric crystals used for acoustic wave applications. He was mostly funded by an Army project.

Name: Cowperthwait, Jacob

Worked for more than 160 Hours: No

Contribution to Project:

Jacob worked on the development of files for the calculation of optimal orientations for surface acoustic wave propagation. He was an NSF
REU student in 2002 and regular undergraduate afterwards, when he inspected orientations in regular acoustic wave crystals and new crystals. His work generated an IEEE 2003 Frequency Control Symposium paper.

Name: Spinney, Patrick

Worked for more than 160 Hours: No

Contribution to Project:

Patrick worked on SAW parameter extraction based on measured device response as an NSF REU student in 2002. He is now a graduate student funded by another colleague in the Dept. of Electrical and Computer Engineering at the University of Maine.

Name: Beaucage, Timothy

Worked for more than 160 Hours: Yes

Contribution to Project:

Tim started as an NSF REU student working on the measurement of crystal density, the design of microfluidic chambers for acoustic wave biosensors, and the extraction of thermal expansion coefficients for acoustic wave crystals. Tim presented his MS thesis on these topics in July 2007. He has been mostly funded by an Army project.

Name: Tkachuk, Vitaly

Worked for more than 160 Hours: No

Contribution to Project:

Vitaly was an NSF REU student involved in this project with one of the graduate student, Thomas Kenny, in the implementation of Green function methods for the determination of orientation of propagation and device modeling.

Name: Jordan, Jared

Worked for more than 160 Hours: No

Contribution to Project:

Jared Jordan was involved in this project as an NSF REU student, and performed measurements of piezoelectric constants and the determination of acoustic wave modes using electromagnetic transducer technology (EMAT). His work generated a conference paper.

Name: Hermansen, Kiva

Worked for more than 160 Hours: No

Contribution to Project:

Kiva was involved in this project under the preparation of samples for acoustic wave measurements (aligning, cutting, grinding, and polishing) and also on the extraction of dielectric constants procedures.

Name: Duy, Stephanie

Worked for more than 160 Hours: No

Contribution to Project:

Stephanie continued the work started by Kiva in sample preparation and dielectric constant extraction. She performed measurement on LGX samples along Z and Y crystalline axis, working together with two graduated students under Prof. Pereira da Cunha advisory, Peter Davulis and Blake Sturtevant.

Technician, Programmer

Name: Moonlight, Thomas

Worked for more than 160 Hours: No

Contribution to Project:

Thomas has been giving technical support regarding equipment maintenance and overseeing material purchase. He has also provided support in equipment and test procedure development. Thomas is mainly funded by an Air Force contract.

Name: Call, Mike

Worked for more than 160 Hours: Yes

Contribution to Project:

Mike has been giving technical support regarding crystal orientation measurements using XRD equipment, equipment maintenance and overseeing material purchase. Mike has been funded by several projects from diverse funding sources.

Name: Bernhardt, George

Worked for more than 160 Hours: Yes

Contribution to Project:

George has been giving technical support mostly in clean room fabrication issues, including photolitography, pattern generation, metal deposition. George is funded by several projects from diverse funding sources.

Other Participant

Research Experience for Undergraduates

Name: Withee, Jason

Worked for more than 160 Hours: No

Contribution to Project:

Jason participated in this project as an NSF REU student during the summer of 2007. He worked closely with Evan Dudzik, one of the graduate students involved in the project, in the design of an acquisition board for capturing the signal coming from a surface acoustic ware wireless passive tag and providing the required digital signal processing.

Years of schooling completed: Junior

Home Institution: Same as Research Site

Home Institution if Other:
Home Institution Highest Degree Granted(in fields supported by NSF): Doctoral Degree
Fiscal year(s) REU Participant supported: 2007
REU Funding: No Info

Organizational Partners

Other Collaborators or Contacts

Peter M. Smith, Associate Dean (Academic)
Faculty of Engineering
McMaster University.

Prof. Dr.-techn. Leonhard M. Reindl
Albert-Ludwig-University of Freiburg
Department of Microsystems Engineering
Laboratory for Electrical Testing

Prof. Donald C. Malocha
University of Central Florida
Orlando, Fl

Activities and Findings

Research and Education Activities:

The research and education activities under this project embrace:
- Graduate student research and training, which include several technical paper presentations by the students in major conferences in the field, namely IEEE International Ultrasonics Symposium, IEEE International Frequency Control Symposium, and IEEE International Sensors Conference (conference papers listed in this report).
- Journal publications with the major findings (publications listed in this report).
- Undergraduate training with 15 NSF REU students being directly advised by the the PI. Ten of these 15 continued to do research with the PI or colleagues, while still undergraduate students. In addition, seven out of those 15 went to graduate school.
- High school activities through GK-12 fellows (graduate students) who brought and included wireless and filtering topics in local high schools.
- Inclusion of proposal and project writing in senior undergraduate courses. The students were asked to write individual proposals for a course project (ECE 466 Sensors and Instrumentation Laboratory).
The proposals were defended to other students. After every student presented a proposal, the class voted the best proposals for group work and implementation (the PI monitored the feasibility regarding the course timeframe).
- Another educational initiative was incorporated in ECE 453 (Microwave Engineering), where students were asked to prepare lab manuals, and execute the envisioned experiments, as if they were preparing classes and training other students. The activity helped prepare students to convey information to others, write appropriate reports, and be initiated in the tasks of working in group on diverse lab experiments. In addition, several of the prepared lab manuals were be used in following course session experiments.
These hands-on learning experience showed very fruitful with very positive feedback from the students.
- Interactions with other Universities, namely University of Central Florida, Magdenburg University (Germany), Albert-Ludwig-University of Freiburg (Germany), on topics including acoustic wave modeling, wireless SAW devices, and wireless sensors and tags.
- Inclusion of high performance commercial Advanced Design System (ADS) software in the ECE 453 Microwave Engineering course taught by the PI, including filter design, antenna design, devices' fabrication and test by undergraduate and graduate students.

Findings:

Major scientific (research) findings include (technical details in the published papers listed in this report):
- Capability of identifying new High Velocity Pseudo Surface Acoustic Wave (HVPSAW), Pseudo Surface Acoustic Wave (PSAW), and Shear Horizontal Surface Acoustic Wave (SH-SAW) orientations in regular (quartz, lithium tantalate, and lithium niobate) and new piezoelectric crystals (potassium niobate, gallium orthophosphate, langasite family of crystal) for high frequency wireless applications and biosensor applications. (technical details described in the listed published conference and peer reviewed papers)

- Capability to model HVPSAW, and PSAW, and SH-SAW propagation and transduction properties, including the excitation, coupling and radiation to spurious bulk acoustic wave modes.
- Capability to model acoustic wave transducer and periodic structures on piezoelectric crystals. The relevance of this modeling reflects on enabling this technology and findings to be used in the design of higher frequency wireless filters and sensors for bio applications (liquid environment). This work is under final stages of completion through two Ph.D. thesis by Tom Kenny and Tom Pollard under the PI's advisory.
- Investigation of computational methods including boundary element method and finite element methods for propagation and structure modeling in finite and infinite structures for acoustic wave modal analysis and device applications.
- Investigation of stiffness variation of polymer film deposited on piezoelectric substrates using surface acoustic wave propagation. The target of the research is to improve shear horizontal mode trapping and device design for biosensor and communication applications.
- Extraction of SAW network model parameters based on the above mentioned finite and boundary element method analyses. This technique allows the necessary tools for fast and accurate design of SAW devices, based on a computation intensive technique.
- Design, fabrication, and implementation of a novel wireless tag sensor device and system using coded matched filters. The developed wireless system employs passive, battery-free SAW devices as sensors. These SAW devices also allow for multisensor interrogation, permitting the monitoring of several individual samples or diverse measurands. The device design and system implementation used the tools developed under this project.

Training and Development:

Research and teaching skills and experience:

- Team work with other graduates, technical staff, and faculty.
- Multidisciplinary approach to research and problem solving, involving expertise from other areas of knowledge (biotechniques, mechanical engineering, chemical, information theory, signal processing, and mathematical techniques).
- Co-advisory of undergraduate students by graduate student (monitored by the PI)
- Technical document writing and publication in peer reviewed journals by graduate and undergraduate students
- Paper presentations in conferences, both oral and poster by graduate and undergraduate students involved in the project
- Microwave equipment specification and purchase by graduate, undergraduate students, and staff.
- Computer network design and parallel operation
- Development of class material for GK-12 fellows for inclusion in local high school classes dealing with wireless and microwave techniques.
- Teaching assistant experience in preparing lab., working with professional software, and teaching undergraduate courses.
- Training, operation, and design of clean room equipment and techniques required for microelectronics fabrication. These techniques are necessary for the previously mentioned research activities involved in acoustic wave modeling, design, and experimental verification.
- Wireless sensor interrogation system design, antenna integration and optimization, and wireless sensor system implementation.

Outreach Activities:

Participation, seminar elaboration, and activities coordination in
- Engineering week at the University of Maine
- Monitor GK-12 fellows and high school activities
- NSF REU through advisory, student competitions
- NSF RET and associated seminars
- Integrative Graduate Education and Research Traineeship (IGERT) programs
- Discussion with visiting parents and students about the importance of STEM research
- Presentation and Laboratory visits to Elementary, Middle School, and High School students throughout the year
- Yearly Graduate and undergraduate EXPO seminars and poster presentations to the University community, visiting sponsors, parents, GK-12 schools, and overall community.

Journal Publications

T.D. Kenny, T.B. Pollard, E. Berkenpas, M. Pereira da Cunha, "FEM/BEM Impedance and Power Analysis for Measured LGS SH-SAW Devices", IEEE Transactions on Ultrasonics, Ferroelectrics, and Frequency Control, p. 402-411, vol. 53, (2006). Published,

T.B. Pollard, T.D. Kenny, J. F. Vetelino, M. Pereira da Cunha, "Pure SH-SAW Propagation, Transduction and Measurements on KNbO3", IEEE Transactions on Ultrasonics, Ferroelectrics, and Frequency Control, p. 199-208, vol. 53, (2006). Published,

J. A. Thiele and M. Pereira da Cunha, "Platinum And Palladium High Temperature Transducers On Langasite", IEEE Transactions on Ultrasonics, Ferroelectrics, and Frequency Control, p. 545-549, vol. 52, (2005). Published,

B. J. Meulendyk, M. C. Wheeler and M. Pereira Da Cunha, "Analyses and Mitigation of Spurious Scattered Signals in Acoustic Wave Reflection Measurements", Nondestructive Testing and Evaluation, p. 155-169, vol. 21, (2006). Published,

E. Berkenpas, S. Bitla, P. Millard, and M. Pereira da Cunha, "Pure Shear Horizontal SAW Biosensor on Langasite", IEEE Trans. Ultrason. Ferroelec. Freq. Contr., p. 1404-1411, vol. 51, (2004). Published,

T. Beaucage, W. Porter, S. Speakman, A. Payzant, E. Beenfeldt, M. Pereira da Cunha, "Comparison Between Bulk and Crystal Lattice Expansion Coefficients of LGT", IEEE Transactions on Ultrasonics Ferroelectrics and Frequency Control, p. , vol. , ( ). Submitted,

J.A. Thiele and M. Pereira da Cunha, "High Temperature LGS SAW Gas Sensor", Sensor and Actuators B: Chemical, p. 246-252, vol. 2005, (113). Published,

L.D. Doucette, M. Pereira da Cunha, R. J. Lad, "Precise Orientation if Single Crystals by a Simple X-Ray Diffraction Rocking Curve Method", Rev. of Scientific Instruments, p. 36106, vol. 76, (2005). Published,

M. Pereira da Cunha, D. C. Malocha, D. R. Puccio, J. Thiele, and T. B. Pollard, "LGX Pure Shear Horizontal SAW for Liquid Sensor Applications", IEEE Sensors Journal, p. 554-561, vol. 03, (2003). Published,

J. A. Thiele and M. Pereira da Cunha, "High Temperature Surface Acoustic Wave Devices: Fabrication And Characterization", Electronics Letters, p. 818-819, vol. 39, (2003). Published,

M. Pereira da Cunha, D.C. Malocha, E.L. Adler, K.J. Casey, "Surface and Pseudo Surface Acoustic Waves in Langatate: Predictions and Measurements", IEEE Trans. Ultrason. Ferroelec. Freq. Contr., p. 1291-1299, vol. 49, (2002). Published,

E. Dudzik, A. Abedi, D. Hummels, and Mauricio Pereira da Cunha, "Wireless multiple access surface acoustic wave coded sensor system", Electronics Letters, p. 775, vol. 44, (2008). Published,

Donald F. McCann, Jason M. McGann, Jesse M. Parks, David J. Frankel, Mauricio Pereira da Cunha, and John F. Vetelino, "A Lateral-Field-Excited LiTaO3 High-Frequency Bulk Acoustic Wave Sensor", IEEE Transactions on Ultrasonics, Ferroelectrics, and Frequency Control, p. 779, vol. 56, (2009). Published,

Blake T. Sturtevant, Peter M. Davulis, Mauricio Pereira da Cunha, "Pulse Echo and Combined Resonance Technicques: A Full Set of LGT Acoustic Wave Constants and Temperature Coefficients", IEEE Transactions on Ultrasonics, Ferroelectrics, and Frequency Control, p. 788, vol. 56, (2009). Published,

Books or Other One-time Publications

T. D. Kenny and M. Pereira da Cunha, "Equivalent Circuit Model and Parameter Extraction for HVPSAW", (2006). Proceedings, Published
Editor(s): Institute of Electrical and Electronic Engineers
Collection: IEEE 2006 International Ultrasonics Symposium Proceedings
Bibliography: IEEE 2006 International Ultrasonics Symposium
Proceedings, Vancouver, Canada, Oct. 03-06, 2006, pp. 363-366.

T. B. Pollard and M. Pereira da Cunha, "Pure Shear Horizontal SAW Network Model for Periodic Structures Including Bulk Scattering", (2006). Proceedings, Published
Editor(s): Institute of Electrical and Electronic Engineers
Collection: IEEE 2006 International Ultrasonics Symposium Proceedings
Bibliography: IEEE 2006 International Ultrasonics Symposium Proceedings, Vancouver, Canada, Oct. 03-06, 2006, pp. 88-91.

Timothy Beaucage, Larryl Matthews, Mauricio Pereira da Cunha, "Optical Differential Dilatometry for the Determination of the Coefficients of Thermal Expansion of Single Crystal Solids", (2006). Proceedings, Published
Editor(s): Institute of Electrical and Electronic Engineers

Collection: IEEE 2006 International Ultrasonics Symposium Proceedings
Bibliography: IEEE 2006 International Ultrasonics Symposium Proceedings, Vancouver, Canada, Oct. 03-06, 2006, pp. 788-791.

B.T. Sturtevant, M. Pereira da Cunha, "BAW Phase Velocity Measurements by Conventional Pulse Echo Techniques with Correction for Couplant Effect", (2006). Proceedings, Published
Editor(s): Institute of Electrical and Electronic Engineers
Collection: IEEE 2006 International Ultrasonics Symposium Proceedings
Bibliography: IEEE 2006 International Ultrasonics Symposium Proceedings, Vancouver, Canada, Oct. 03-06, 2006, pp. 2261-2264.

T.R. Beaucage, E.P. Beenfeldt, S.A. Speakman, W.D. Porter, E.A. Payzant, and M. Pereira da Cunha, "Comparison of High Temperature Crystal Lattice and Bulk Thermal Expansion Measurements of LGT Single Crystal", (2006). Proceedings, Published
Editor(s): Institute of Electrical and Electronic Engineers
Collection: IEEE 2006 Frequency Control Symp. Proceedings
Bibliography: IEEE 2006 Frequency Control Symp. Proceedings, Miami, June 04-07, Miami, FL, USA, 2006, pp. 658-663. (PAPER WAS AMONG THE 4 FINALISTS COMPETING FOR BEST STUDENT PAPER AWARD IN THE

P. Davulis, J. A. Kosinski, and M. Pereira da Cunha, "GaPO4 Stiffness and Piezoelectric Constants Measurements using the Combined Thickness Excitation and Lateral Field Technique", (2006). Proceedings, Published
Editor(s): Institute of Electrical and Electronic Engineers
Collection: IEEE 2006 Frequency Control Symp. Proceedings
Bibliography: IEEE 2006 Frequency Control Symp. Proceedings, Miami, June 04-07, FL, USA, 2006, pp. 664-669.

E. Berkenpas, P. Millard, M. Pereira da Cunha, "Novel O157:H7 E. coli Detector Utilizing a Langasite Surface Acoustic Wave Device", (2005). Proceedings, Published
Editor(s): Institute of Electrical and Electronic Engineers

Collection: IEEE International Sensor 2005 Conference
Bibliography: IEEE International Sensor 2005 Conference, Irvine, CA, October 31 ? Nov. 03, 2005. (PAPER WAS AMONG THE 10 FINALISTS COMPETING FOR BEST STUDENT PAPER AWARD IN THE SYMPOSIUM).

Maurício Pereira da Cunha and Jared W. Jordan, "Improved Longitudinal EMAT Transducer for Elastic Constant Extraction", (2005). Proceedings, Published
Editor(s): Institute of Electrical and Electronic Engineers
Collection: 2005 Joint IEEE International Frequency Control Symposium and Precise Time and Interval (PTTI) Systems and Applications Meeting
Bibliography: 2005 Joint IEEE International Frequency Control Symposium and Precise Time and Interval (PTTI) Systems and Applications Meeting, Vancouver, Ca, Aug. 29-31, 2005, pp. 426-432.

B. J. Meulendyk and M. Pereira da Cunha,, "Significance of Power Flow Angle Interference Due to Finite Sample Dimension in Reflection Measurements", (2005). Proceedings, Published
Editor(s): Institute of Electrical and Electronic Engineers

Collection: 2005 Joint IEEE International Frequency Control Symposium and Precise Time and Interval (PTTI) Systems and Applications Meeting
Bibliography: 2005 Joint IEEE International Frequency Control Symposium and Precise Time and Interval (PTTI) Systems and Applications Meeting, Vancouver, Ca, Aug. 29-31, 2005, pp. 164-170.

T. D. Kenny and M. Pereira da Cunha, "Identification Of New LTO HVPSAW Orientations Considering Finite Thickness Electrodes", (2005). Proceedings, Proceedings
Editor(s): Institute of Electrical and Electronic Engineers
Collection: IEEE 2005 International Ultrasonics Symposium Proceedings
Bibliography: IEEE 2005 International Ultrasonics Symposium Proceedings, Rotterdam, the Netherlands, Sept. 18-21, 2005, pp. 2305-2308. (THIS PAPER WAS AMONG THE 3 FINALISTS FOR BEST STUDENT PAP

E. Berkenpas, P. Millard, M. Pereira da Cunha, "A Langasite SH SAW O157:H7 E. coli Sensor", (2005). Proceedings, Published
Editor(s): Institute of Electrical and Electronic Engineers
Collection: IEEE 2005 International Ultrasonics Symposium Proceedings
Bibliography: IEEE 2005 International Ultrasonics Symposium Proceedings, Rotterdam, the Netherlands, Sept. 18-21, 2005, pp. 54-57.

T. B. Pollard and M. Pereira da Cunha, "Improved Pure Shsaw Transduction Efficiency on LGS Using Finite Thickness Gratings", (2005). Proceedings, Published
Editor(s): Institute of Electrical and Electronic Engineers
Collection: IEEE 2005 International Ultrasonics Symposium Proceedings
Bibliography: IEEE 2005 International Ultrasonics Symposium Proceedings, Rotterdam, the Netherlands, Sept. 18-21, 2005, pp. 1048-1051.

N. Saldanha, D. Puccio, M. Pereira da Cunha*, and D.C. Malocha, "Experimental and Predicted TCD and SAW Parameters on LGT [0, 132, Ψ] Substrates", (2005). Proceedings, Published
Editor(s): Institute of Electrical and Electronic Engineers
Collection: IEEE 2005 International Ultrasonics Symposium Proceedings
Bibliography: IEEE 2005 International Ultrasonics Symposium Proceedings, Rotterdam, the Netherlands, Sept. 18-21, 2005, pp. 918-921.

J. A. Thiele and M. Pereira da Cunha, "Dual Configuration High Temperature Hydrogen Sensor On LGS SAW Devices", (2004). Proceedings, Published
Editor(s): Institute of Electrical and Electronic Engineers
Collection: IEEE 2004 International Ultrasonics Symposium Proceedings
Bibliography: IEEE 2004 International Ultrasonics Symposium Proceedings, Aug. 23-27, 2004, Montreal, CA, pp. 809-812. (THIS PAPER RECEIVED THE BEST STUDENT PAPER AWARD FROM THE IEEE 2004 SYMPOSI

T. B. Pollard, Thomas D. Kenny, and M. Pereira da Cunha, "SH-SAW Transducer Analysis on Single Crystal KNbO3 for Liquid Sensors", (2004). Proceedings, Published
Editor(s): Institute of Electrical and Electronic Engineers
Collection: IEEE 2004 International Ultrasonics Symposium Proceedings
Bibliography: IEEE 2004 International Ultrasonics Symposium Proceedings, Aug. 23-27, 2004, Montreal, CA, pp. 390-395. (THIS PAPER WAS AMONG THE 4 FINALISTS COMPETING FOR THE BEST STUDENT PAPER A

T.D. Kenny, T.B. Pollard, E. Berkenpas, M. Pereira da Cunha, "FEM/BEM Impedance And Power Analysis For Measured LGS SH-SAW Devices", (2004). Proceedings, Published
Editor(s): Institute of Electrical and Electronic Engineers
Collection: IEEE 2004 International Ultrasonics Symposium Proceedings
Bibliography: IEEE 2004 International Ultrasonics Symposium Proceedings, Aug. 23-27, 2004, Montreal, CA, pp. 1371-1374. (THIS PAPER WAS ALSO AMONG THE 4 FINALISTS COMPETING FOR THE BEST STUDENT

E. Berkenpas, S. Bitla, P. Millard, and M. Pereira da Cunha, "Shear Horizontal SAW Biosensor on Langasite", (2003). Proceedings, Published
Editor(s): Institute of Electrical and Electronic Engineers
Collection: Proceedings of the 2003 IEEE Sensors
Bibliography: Proceedings of the 2003 IEEE Sensors, Toronto, CA, Oct. 2003, pp. 661-664.

J. A. Thiele and M. Pereira da Cunha, "High Temperature SAW Gas Sensor on Langasite", (2003). Proceedings, Published
Editor(s): Institute of Electrical and Electronic Engineers
Collection: Proceedings of the 2003 IEEE Sensors
Bibliography: Proceedings of the 2003 IEEE Sensors, Toronto, CA, Oct. 2003, pp. 769-772.

M. Pereira da Cunha, T.B. Pollard, H. Whitehouse, and P.M. Worsch, "GaPO4 SAW Devices: Measured and Predicted Propagation Properties", (2003). Proceedings, Published
Editor(s): Institute of Electrical and Electronic Engineers
Collection: IEEE 2003 International Ultrasonics Symposium Proceedings
Bibliography: IEEE 2003 International Ultrasonics Symposium Proceedings, October 5-8, Honolulu, Hawaii, 2003, pp. 110-113.

T. B. Pollard, J. F. Vetelino, and M. Pereira da Cunha, "Pure SH SAW On Single Crystal Knbo3 For Liquid Sensor Applications", (2003). Proceedings, Published
Editor(s): Institute of Electrical and Electronic Engineers
Collection: IEEE 2003 International Ultrasonics Symposium Proceedings
Bibliography: IEEE 2003 International Ultrasonics Symposium Proceedings, October 5-8, Honolulu, Hawaii, 2003, pp. 1125-1128.

E. Berkenpas, S. Bitla, P. Millard, and M. Pereira da Cunha, "LGS Shear Horizontal SAW Devices for Biosensor Applications", (2003). Proceedings, Published
Editor(s): Institute of Electrical and Electronic Engineers
Collection: IEEE 2003 International Ultrasonics Symposium Proceedings
Bibliography: IEEE 2003 International Ultrasonics Symposium Proceedings, October 5-8, Honolulu, Hawaii, 2003, pp. 1404-1407.

J. A. Thiele and M. Pereira da Cunha, "High Temperature LGS SAW devices with Pt/WO3 and Pd Sensing Films", (2003). Proceedings, Published
Editor(s): Institute of Electrical and Electronic Engineers
Collection: IEEE 2003 International Ultrasonics Symposium Proceedings
Bibliography: IEEE 2003 International Ultrasonics Symposium Proceedings, October 5-8, Honolulu, Hawaii, 2003, pp. 1750-1753.

J.A. Cowperthwaite and M. Pereira da Cunha, "Optimal Orientation Function For SAW Devices", (2003). Proceedings, Published
Editor(s): Institute of Electrical and Electronic Engineers
Collection: IEEE 2003 Frequency Control Symp. Proceedings
Bibliography: IEEE 2003 Frequency Control Symp. Proceedings, pp. 881-887, May 05-08, Tampa, FL, USA, 2003.

M. Pereira da Cunha, D. C. Malocha, R. Puccio, J. Thiele, and T. Pollard, "High Coupling, Zero TCD SH Wave on LGX", (2002). Proceedings, Published
Editor(s): Institute of Electrical and Electronic Engineers
Collection: IEEE 2002 International Ultrasonics Symposium Proceedings
Bibliography: IEEE 2002 International Ultrasonics Symposium Proceedings,October 8-11, Munich, Germany, 2002, pp. 368-371.

M. Pereira da Cunha, D. C. Malocha, R. Puccio, and J. Thiele, "LGX Pure Shear Horizontal SAW for Liquid Sensor Applications", (2002). Proceedings, Published
Editor(s): Institute of Electrical and Electronic Engineers
Collection: Proceedings of the 2002 IEEE Sensors
Bibliography: Proceedings of the 2002 IEEE Sensors, pp. 1165-1170, Orlando, FL, June 2002.

M. Pereira da Cunha, T. Moonlight, R. Lad, G. Bernhardt, D. J. Frankel, "Enabling Very High Temperature Acoustic Wave Devices for Sensor & Frequency Control Applications
", (2007). Proceedings, Published
Editor(s): Institute of Electrical and Electronic Engineers
Collection: IEEE 2007 International Ultrasonics Symposium Proceedings
Bibliography: IEEE 2007 International Ultrasonics Symposium
Proceedings, New York, U.S.A., Oct. 03-06, 2007, pp. 2107-2110.

P. M. Davulis, B. T. Sturtevant, S. I. Duy, M. Pereira da Cunha, "Revisiting LGT dielectric constants and temperature coefficients up to 120 deg. C", (2007). Proceedings, Published
Editor(s): Institute of Electrical and Electronic Engineers
Collection: IEEE 2007 International Ultrasonics Symposium Proceedings

IEEE 2007 International Ultrasonics Symposium
Proceedings, New York, U.S.A.

Bibliography: IEEE 2007 International Ultrasonics Symposium
Proceedings, New York, U.S.A., Oct. 03-06, 2007, pp. 1397-1400.

T. D. Kenny, B. J. Meulendyk, and M. Pereira da Cunha, "Novel SAW Network Model Parameter Extraction Technique", (2007). Proceedings, Published
Editor(s): Institute of Electrical and Electronic Engineers
Collection: IEEE 2007 International Ultrasonics Symposium Proceedings
Bibliography: IEEE 2007 International Ultrasonics Symposium
Proceedings, New York, U.S.A., Oct. 03-06, 2007, pp. 2343-2146.

Evan Dudzik, Ali Abedi, Donald Hummels, Mauricio Pereira da Cunha, "Orthogonal Code Design for Passive Wireless Sensors", (2008). Proceedings, Published
Editor(s): Institute of Electrical and Electronic Engineers
Collection: 24th Biennial Symposium on Communications
Bibliography: Kingston, Ontario, Canada, Jun. 24-26.

D.J. Frankel, G.P. Bernhardt, B.T. Sturtevant, T. Moonlight, M. Pereira da Cunha, R.J. Lad, "Stable Electrodes and Ultrathin Passivation Coatings
for High Temperature Sensors in Harsh Environments", (2008). Proceedings, Published
Editor(s): Intitute of Electrical and Electronic Engineers (IEEE)
Collection: IEEE International Sensor 2008 Conference Proceedings
Bibliography: Lecce, Italy, October 26 ? 29, pp.82-85

M. Pereira da Cunha, T. Moonlight, R. Lad, D. Frankel, G. Bernhardt, "High Temperature Sensing Technology for Applications Up To 1000°C", (2008). Proceedings, Published
Editor(s): Intitute of Electrical and Electronic Engineers (IEEE)

Collection: IEEE International Sensor 2008 Conference Proceedings
Bibliography: Lecce, Italy, October 26 ? 29, pp.752-755.

Peter Davulis, Amit Shyam, Edgar Lara-Curzio, Mauricio Pereira da Cunha, "High Temperature Elastic Constants of Langatate from RUS Measurements up to 1100°C", (2008). Proceedings, Published
Editor(s): Intitute of Electrical and Electronic Engineers (IEEE)

Collection: IEEE 2008 International Ultrasonics Symposium Proceedings
Bibliography: Beijing, China, Nov. 02-05, pp.2150-2153.

Evan Dudzik, Ali Abedi, Donald Hummels, Mauricio Pereira da Cunha, "Wireless Sensor System Based on SAW Coded Passive Devices for Multiple Access", (2008). Proceedings, Published
Editor(s): Intitute of Electrical and Electronic Engineers (IEEE)

Collection: IEEE 2008 International Ultrasonics Symposium Proceedings
Bibliography: Beijing, China, Nov. 02-05, pp.1116-1119.

M. Pereira da Cunha, R. Lad, T. Moonlight, G. Bernhardt, D. Frankel, "High Temperature Stability of Langasite Surface Acoustic Wave Devices", (2008). Proceedings, Published
Editor(s): Intitute of Electrical and Electronic Engineers (IEEE)

Collection: IEEE 2008 International Ultrasonics Symposium Proceedings
Bibliography: Beijing, China, Nov. 02-05, pp. 205-208.

Jeremy A. Thiele, "High Temperature LGX Acoustic Wave Devices and Applications for Gas Sensor", (2005). Thesis, Published
Editor(s): the University of Maine
Collection: MSc. in Electrical Engineering
Bibliography: the University of Maine Graduate School

Eric J. Berkenpass, "Investigation Of Langasite Pure Shear Horizontal Surface Acoustic Wave Biosensors", (2005). Thesis, Published
Editor(s): the University of Maine
Collection: MSc. in Electrical Engineering
Bibliography: Graduate School, the University of Maine

Timothy R. Beaucage, "High Temperature LGT Expansion Measurements Through Multiple Techniques", (2007). Thesis, Published
Editor(s): the University of Maine
Collection: MSc. in Electrical Engineering
Bibliography: Graduate School, the University of Maine

Thomas Kenny, "Identification and Modeling of New HVPSAW Orientations Considering Finite Thickness Electrodes", (2009). Thesis, Submitted
Editor(s): the University of Maine
Collection: Ph.D. in Electrical Engineering
Bibliography: Graduate School, the University of Maine

Thomas B. Pollard, "Modeling, Fabrication, and Experimental Analysis of Pure Shear Horizontal Surface Acoustic Wave Liquid-Phase Sensor Platforms", (2009). Thesis, Submitted
Editor(s): the University of Maine
Collection: Ph.D. in Electrical Engineering
Bibliography: Graduate School, the University of Maine

Blake Sturtevant, "Characterization of Single Crystal Langatate for Acoustic Wave Applications", (2009). Thesis, Submitted
Editor(s): the University of Maine
Collection: Ph.D. in Physics
Bibliography: Graduate School, the University of Maine

Evan Dudzik, "Wireless Interrogation System Using Passive Surface Acoustic Wave Coded Sensors", (2009). Thesis, Submitted
Editor(s): the University of Maine
Collection: MSc. in Electrical Engineering
Bibliography: Graduate School, the University of Maine

Peter Davulis, "Characterization of the elastic, piezoelectric, and dielectric properties of langatate (LGT) at high temperatures (up to 1100ºC)", ( ). Thesis, ongoing work, defense expected in 2010.
Editor(s): the University of Maine
Collection: Ph.D. in Electrical Engineering
Bibliography: Graduate School, the University of Maine

Web/Internet Site

Other Specific Products

Contributions

Contributions within Discipline:

Major contributions within discipline include (technical details in the papers listed in this report):
- Identification of new High Velocity Pseudo Surface Acoustic Wave (HVPSAW), Pseudo Surface Acoustic Wave (PSAW), and Shear Horizontal Surface Acoustic Wave (SH-SAW) orientations in regular (quartz, lithium tantalate, and lithium niobate) and new piezoelectric crystals (potassium niobate, gallium orthophosphate, langasite family of crystal) for high frequency wireless applications and biosensor applications.
- Modeling of HVPSAW, and PSAW, and SH-SAW propagation and transduction properties, including the excitation, coupling and radiation to spurious bulk acoustic wave modes.
- Modeling of acoustic wave transducer and periodic structures on piezoelectric crystals. The relevance of this modeling reflects on enabling this technology and findings to be used in the design of higher frequency wireless filters and sensors for bio applications (liquid environment).
- Investigation of computational methods including boundary element method and finite element methods for propagation and structure modeling in finite and infinite structures for acoustic wave modal analysis and device applications.
- Investigation on piezoelectric crystal properties, orientations, and electrode thin film for wireless and sensor applications
- Investigation of passive wireless sensor systems using novel thin film electrode materials, piezoelectric crystals, and orientations researched.

Contributions to Other Disciplines:

The contributions within discipline previously described have impacted other fields of knowledge, namely the sensors, harsh environment devices for frequency control, and characterization of acoustic wave crystals. The impact is partially verified through the related publications attached to this report and also through contemporary work of other authors in the research of the gallium orthophosphate, potassium niobate, and the langasite family of crystals for high temperature sensors, liquid sensors, and material characterization. These publications can be found in different conferences' proceeding and journals, such as in the proceeding of the IEEE Ultrasonics Symposia, IEEE Frequency Control Symposia, and the IEEE Transactions on Ultrasonics, Ferroelectrics, and Frequency Control.

Contributions to Human Resource Development:

This NSF Career project has been instrumental in providing research opportunities and scientific dissemination in the State of Maine through:
- Seven NSF REU Career students, five of which have become graduate students in Maine with the PI or one of his colleagues
- Training of local technicians and scientific personnel in acoustic wave device modeling and fabrication
- Participation in the NSF GK-12 program, through which the findings and training of graduate students have been brought to local high schools in Maine
- Participation in the NSF RET program, exposing the topics of the Career project to local Maine high school teachers, enabling their training during high school holidays, and ultimately bringing research topics to high school students.
- Integration with the Sensor NSF IGERT program at University of Maine, bringing multidisciplinary approach to the Career findings in terms of modeling, new piezoelectric materials research, and identification of new propagation modes.
- Enabling other successful proposals to be written and granted to the PI and co-workers in the areas of wireless communication, sensors, and material research, thus generating further personnel training to the State of Maine and to the country.

Contributions to Resources for Research and Education:

This NSF Career project has greatly facilitated the establishment of the Microwave Acoustic Laboratory (MAL) at the Department of Electrical and Computer Engineering and at the Laboratory for Surface Science and Engineering, the University of Maine. Through the MAL and the finding associated with this CAREER project in acoustic wave propagation calculation and device modeling, several other projects have been facilitated, including new piezoelectric crystals research and characterization, thin film research for acoustic wave device, gas sensor research, and biosensor research and device modeling.

The facilities put together in this project, in particular the generation of a computer cluster for the calculation of the finite element modeling used in the calculation of acoustic wave propagation and device modeling, granted the means and the environment for twelve graduate students and twenty seven undergraduate students under the direct advisory of the PI to develop their work. In addition, these facilities permit the interactions and platform to the work of high schools teachers, GK-12 fellows, the preparation of undergraduate microwave (ECE 453 Microwave Engineering) and Sensor lab (ECE 466 Sensor Laboratory and Instrumentation) courses thought by the PI with the assistance of his graduate students.

Contributions Beyond Science and Engineering:

As a result of this CAREER project, the PI has established contacts with companies and national laboratories interested in the outcomes of the project in terms of the identification of new propagation modes, acoustic wave device modeling, and new materials research. These companies and national laboratories are: Luna Innovations, VA; Vectron Inc., NH; RF Micro Devices, NC; Applied Sensor Research & Development Corporation, MD; the Oak Ridge National Laboratory; the Naval Undersea Warfare Center, RI; and the Air Force Research Laboratory, OH. The mentioned companies and national laboratories have also been interested and actively recruiting the graduate and undergraduate students trained by the PI under this project.

Conference Proceedings

Categories for which nothing is reported:

Organizational Partners

Any Web/Internet Site

Any Product

Any Conference

FEM/BEM Impedance and Power Analysis for Measured LGS SH-SAW Devices

Thomas D. Kenny, *Student Member, IEEE*, Thomas B. Pollard, *Student Member, IEEE*, Eric Berkenpas, *Student Member, IEEE*, and Mauricio Pereira da Cunha, *Senior Member, IEEE*

***Abstract*—Pure shear horizontal piezoelectrically active surface and bulk acoustic waves (SH-SAW and SH-BAW) exist along rotated Y-cuts, Euler angles (0°, θ, 90°), of trigonal class 32 group crystals, which include the LGX family of crystals (langasite, langatate, and langanite). In this paper both SH-SAW and SH-BAW generated by finite-length, interdigital transducers (IDTs) on langasite, Euler angles (0°, 22°, 90°), are simulated using combined finite- and boundary-element methods (FEM/BEM). Aluminum and gold IDT electrodes ranging in thickness from 600 Å to 2000 Å have been simulated, fabricated, and tested, with both free and metalized surfaces outside the IDT regions considered. Around the device's operating frequency, the percent difference between the calculated IDT impedance magnitude using the FEM/BEM model and the measurements is better than 5% for the different metal layers and thicknesses considered. The proportioning of SH-SAW and SH-BAW power is analyzed as a function of the number of IDT electrodes; type of electrode metal; and relative thickness of the electrode film, h/λ, where λ is the SH-SAW wavelength. Simulation results show that moderate mechanical loading by gold electrodes increases the proportion of input power converted to SH-SAW. For example, with a split-electrode IDT, comprising 238 electrodes with a relative thickness $h/\lambda = 0.63\%$ and surrounded by an infinitesimally thin conducting film, nearly 9% more input power is radiated as SH-SAW when gold instead of aluminum electrodes are used.**

I. Introduction

The pure shear horizontal (SH) surface acoustic waves (SAW) that occur on rotated Y-cuts, Euler angles (0°, θ, 90°), of the LGX family of crystals (langasite, LGS; langatate, LGT; and langanite, LGN) have been identified as having several attractive features for SAW device applications [1]–[5]. High frequency filtering, biological sensing, and liquid properties sensing are among these potential SAW applications along selected LGX substrate orientations, due to properties such as: higher phase velocity than the regular SAW or Rayleigh mode, which makes it suited for higher frequency devices; reduced attenuation compared to other SAW and PSAW modes when the surface is immersed in liquid, which can be used for liquid and biosensor applications; calculated and measured electromechanical coupling up to 0.8%; and slightly greater power penetration depth in comparison to the Rayleigh SAW mode, when a grating or thin metallic film is used for additional guidance of the SH-SAW at the surface. This latter property, namely the use of a uniform metallic film, is discussed and explored in this work to increase the proportion of input power converted to SH-SAW by the interdigital transducers (IDT) along LGS propagation directions of interest. For liquid sensor applications, the thin metallic film is used to isolate the device response from variations in the electrical properties of the liquid media [4].

Over the past three decades, boundary-element method (BEM) and finite-element method (FEM) techniques have been applied to the simulation of SAW devices. A rigorous BEM analysis of acoustical and electrical fields generated by IDTs was discussed in [6], which considered in particular the SH-SAW cut of PZT-4 Euler angles (0°, 90°, 0°). Finite-element techniques have been used more recently to perform full IDT analysis [7] and to incorporate the effect of mass loading due to the finite mass of the IDT electrodes into the BEM analysis, in the generation of SAW, pseudo-SAW [8]–[10], and SH-SAW [11]–[13].

Both finite structures [9], [10] and infinite periodic electrode structures [8], [11], [13] have been considered. In the case of infinite periodic electrode grating structures, the calculated dispersion curves have been used to extract modeling parameters, such as coupling of modes (COM) parameters [8] and network parameters [7].

This work reports on numerical simulations, using combined FEM/BEM techniques, and experimental results regarding the generation of SH-SAW and SH-BAW by finite-length IDTs along rotated Y-cut langasite, Euler angles (0°, 22°, 90°). This work also investigates the effect of mass loading by different metal types and thicknesses of IDT electrodes on the percentage of input power converted to SH-SAW, or the SH-SAW transduction efficiency. High transduction efficiency is critical for high performance, low-loss devices, with low spurious levels, and improved signal-to-noise ratio in the case of liquid sensors. Aluminum and gold IDT electrodes ranging in thickness from 600 Å to 2000 Å have been simulated, fabricated, and tested, with both free and metalized surfaces considered outside the IDT regions. Around the device's operating frequency, the percent difference between calculated IDT impedance using the FEM/BEM model and the measurements is better than 5% for the different metal layers and thicknesses considered. The simulations performed have shown that, for the LGS propagation direction considered,

Manuscript received December 10, 2004; accepted August 20, 2005. This work was conducted with support from the National Science Foundation (grants ECS-0233463 and ECS-0134335).

The authors are with the Department of Electrical and Computer Engineering, University of Maine, Orono, ME (e-mail: mdacunha@eece.maine.edu).

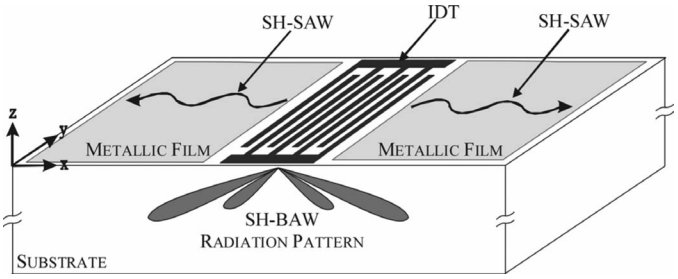

Fig. 1. Structure considered and coordinate system adopted.

virtually all input power is converted to SH-BAW—and thus none to SH-SAW—when regions outside of the IDT are electrically free, regardless of the number of IDT electrodes, electrode metal type, and electrode layer thickness. In contrast, SH-SAW transduction efficiency of up to 72% has been predicted when the IDTs are surrounded by an infinitesimally thin conducting film. The analysis performed discusses the SH-BAW and SH-SAW power partition both as a function of the wave propagation vector, or $\boldsymbol{k}$-vector, and as a function of the angle inside the substrate.

Section II describes the theoretical background of the FEM/BEM IDT model implemented in this work. Section III presents numerical and experimental results regarding the partitioning of input power between SH-SAW and SH-BAW modes, the distribution of SH-BAW power within the substrate, and the comparison between calculated and measured IDT responses. Section IV is devoted to the conclusions.

II. Theoretical Background

The structure and coordinate system considered in this analysis are illustrated in Fig. 1. The IDT is patterned on the surface of a piezoelectric substrate that occupies the half-space $z < 0$. Surface regions outside of the IDT are considered free of mechanical stress, though they may be covered with an infinitesimally thin conducting layer. The fields associated with each surface or bulk wave mode are assumed to follow $\boldsymbol{F}(x,z,t) = \boldsymbol{\tau}(k_x,z)e^{j(\omega t - k_x x)}$, where ω is the angular frequency, k_x is the wave-vector component parallel to the surface, and the function $\boldsymbol{\tau}(k_x,z)$ is the weighted sum of complex exponentials describing how $\boldsymbol{F}$ varies with depth. Surface waves propagate along $\pm x$ rotated directions. No field variation is assumed in the direction normal to the sagittal plane (i.e., $\partial/\partial y = 0$), and the phasor notation will be adopted from this point forward.

A. Spectrum of Waves

Applying a sinusoidal varying electric potential to IDT structures in piezoelectric solids generate a combination of surface and bulk acoustic waves, usually referred to as a "spectrum of waves" [6]–[13]. The knowledge of how the input electrical power distributes among the acoustical modes allows a better understanding of the IDT performance, which leads to improved modeling, and ultimately to the design of efficient transducers for a particular mode.

The pure SH-SAW orientation considered in this paper is a particular symmetry case, classified as symmetry Type 4 in [14], in which the sagittal mechanical particle displacement components uncouple from the electrical field and the shear horizontal mechanical particle displacement component, leading to two separate solutions. One solution is a purely mechanical sagittal wave, and the other solution is the piezoelectrically stiffened pure SH wave [15]. The fields used in the matrix method [16] to solve the acoustic wave problems along symmetry Type 4 orientations are the surface normal component of stress, T_4; particle velocity, ν_2; surface normal component of electric displacement, D_3; and electric potential, ϕ, arranged in the vector $\boldsymbol{\tau} = [T_4 \;\; D_3 \;\; \nu_2 \;\; j\omega\phi]^T$, where the superscript "T" indicates transpose. The dependency of $\boldsymbol{\tau}$ with z is given by $(\partial\boldsymbol{\tau}/\partial z) = j\omega[\boldsymbol{A}]\boldsymbol{\tau}$, where the system matrix $[\boldsymbol{A}]$, defined in (1), is a function of slowness, $s_x = k_x/\omega$, mass density, ρ, and rotated stiffness, piezoelectric, and permittivity constants, c_{hijk}, e_{ijk}, and ε_{ik}, respectively [16]:

$$[\boldsymbol{A}] = \begin{bmatrix} s_x\left[\boldsymbol{\Gamma}^{13}\right][\boldsymbol{X}] & [\boldsymbol{g_0}] - s_x^2\left\{\left[\boldsymbol{\Gamma}^{11}\right] - \left(\boldsymbol{\Gamma}^{13}\right)[\boldsymbol{X}]\left[\boldsymbol{\Gamma}^{31}\right]\right\} \\ [\boldsymbol{X}] & s_x[\boldsymbol{X}]\left[\boldsymbol{\Gamma}^{31}\right] \end{bmatrix}, \tag{1}$$

where, for the particular symmetry 4 case:

$$\left[\boldsymbol{\Gamma}^{ik}\right] = \begin{bmatrix} c_{2i2k} & e_{k2i} \\ e_{i2k} & -\varepsilon_{ik} \end{bmatrix} \quad [\boldsymbol{X}] = \left[\boldsymbol{\Gamma}^{33}\right]^{-1} \quad [\boldsymbol{g}_o] = \begin{bmatrix} \rho & 0 \\ 0 & 0 \end{bmatrix}. \tag{2}$$

B. Partial Mode Selection

At any single angular frequency, ω, it is possible to express $\boldsymbol{\tau}$ as a function of k_x using normal-mode expansion of the eigenvectors and eigenvalues of $j[\boldsymbol{A}]$ [16] as in:

$$\boldsymbol{\tau}\,(k_x, z<0) = [\boldsymbol{P}]\begin{bmatrix} e^{\omega\gamma_1 z} & 0 \\ 0 & e^{\omega\gamma_2 z} \end{bmatrix}\boldsymbol{c}, \tag{3}$$

where $[\boldsymbol{P}]$ is the 4×2 matrix containing 2 eigenvectors of $j[\boldsymbol{A}]$, γ_1 and γ_2 are the corresponding eigenvalues, and $\boldsymbol{c}$ is the 2×1 normal-mode weighting vector. Although the matrix $j[\boldsymbol{A}]$ has four eigenvectors, only those partial modes that decay with depth and those that radiate power into the lower half space [17] occupied by the substrate are selected to address any propagating mode, and consequently, to build $\boldsymbol{\tau}(k_x)$. For the coordinate system adopted, eigenvalues with positive real parts correspond to partial modes that decay with depth, herein called decaying partial modes. Purely imaginary eigenvalues correspond instead to radiating modes, or bulk waves. The $\boldsymbol{k}$-vector of the i^{th} bulk wave, $\boldsymbol{k_i}$, is given by:

$$\boldsymbol{k_i} = k_x\hat{\boldsymbol{x}} + k_z\hat{\boldsymbol{z}} = \omega s_x\hat{\boldsymbol{x}} + j\omega\gamma_i\hat{\boldsymbol{z}}, \tag{4}$$

where $\gamma_i(s_x)$ is the i^{th} purely imaginary eigenvalue of $j[\boldsymbol{A}]$ and $\hat{\boldsymbol{x}}$ and $\hat{\boldsymbol{z}}$ are unit vectors in the rotated coordinate system. The Poynting vector [18] of each bulk wave is examined to determine the direction of power flow, and the radiating modes that carry power downward toward the bulk of the crystal are selected.

C. Spectral Domain Green's Functions

In this section, surface normal stress, T_4, and charge, σ, are considered the source of all waves. The dependent variables are represented by the particle displacement, u_2, and surface potential, ϕ. From an electrical standpoint, the electrodes are considered infinitesimally thin sheets of charge located at the surface of the substrate, and the surface charge density, σ is equal to the divergence of the electric displacement evaluated at $z = 0$. Applying Laplace's equation in the vacuum region above the substrate and calculating the divergence of D_3, one obtains:

$$\sigma\left(k_x, z=0\right) = \varepsilon_0 \omega \left|s_x\right| \phi\left(k_x, z=0\right) - D_3\left(k_x, z=0^-\right). \tag{5}$$

It is now possible to write the four-component vector $\boldsymbol{\tau}_\sigma = [T_4\ \sigma\ \nu_2\ j\omega\phi]^T$ at the surface in terms of the modified eigenvector matrix, $[\boldsymbol{P}_\sigma]$:

$$\boldsymbol{\tau}_\sigma\left(k_x, z=0\right) = \left[T_4\ \sigma\ \nu_2\ j\omega\phi\right]^T = \left[\boldsymbol{P}_\sigma\right] \boldsymbol{c}\left(k_x\right), \tag{6}$$

where:

$$\left[\boldsymbol{P}_\sigma\right] = \begin{bmatrix} [\boldsymbol{P}(1,:)] \\ -j\varepsilon_0 \left|s_x\right| [\boldsymbol{P}(4,:)] - [\boldsymbol{P}(2,:)] \\ [\boldsymbol{P}(3:4,:)] \end{bmatrix}, \tag{7}$$

with $[\boldsymbol{P}(1,:)]$, $[\boldsymbol{P}(4,:)]$, and $[\boldsymbol{P}(2,:)]$ indicating the matrices containing the 1st, the 4th, and the 2nd rows of $[\boldsymbol{P}]$, respectively, and $[\boldsymbol{P}(3:4,:)]$ the matrix containing 3rd and 4th rows of $[\boldsymbol{P}]$, a notation adopted from the MATLAB™ Software (The Mathworks, Inc., Natick, MA 01760). Manipulating (6), it is possible to express the surface potential and particle displacement in terms of surface stress, charge density, and the spectral domain Green's functions as in:

$$u_2 = \frac{\Gamma_{uT}}{\omega} T_4 + \frac{\Gamma_{u\sigma}}{\omega} \sigma, \tag{8}$$

$$\phi = \frac{\Gamma_{\phi T}}{\omega} T_4 + \frac{\Gamma_{\phi\sigma}}{\omega} \sigma, \tag{9}$$

where:

$$\begin{bmatrix} \Gamma_{uT} & \Gamma_{u\sigma} \\ \Gamma_{\phi T} & \Gamma_{\phi\sigma} \end{bmatrix} = \frac{\left[\boldsymbol{P}_\sigma(3:4,:)\right] \left[\boldsymbol{P}_\sigma(1:2,:)\right]^{-1}}{j}. \tag{10}$$

Expressions (8) and (9) permit the calculation of the SH wave particle displacement and potential as a function of the distributed electrical charges and mechanical sources located at the surface. An additional equation relating particle displacement and surface stress is obtained next with the aid of FEM techniques, such that (8) and (9) may be combined, yielding a single equation relating electrical potential and surface charge density, including the effect of mass loading.

D. Finite-Element Method

In this work, FEM was applied to relate traction forces and particle displacements at the boundary between the isotropic metallic electrodes and the piezoelectric substrate. Each electrode was divided into discrete elements using a mesh of several linear triangle finite elements. All simulations presented in this work were carried out using triangular elements no wider than $1/64^{\text{th}}$ of the SH-SAW wavelength and with a height-to-width ratio of no greater than 8. Galerkin's method [19] was applied to obtain a system of equations relating the reaction forces, $\boldsymbol{f}$, at each node of the finite-element mesh as $\boldsymbol{f} = \left([\boldsymbol{K}] - \omega^2[\boldsymbol{M}]\right)\boldsymbol{u} = [\boldsymbol{Z}]\boldsymbol{u}$, where the matrices $[\boldsymbol{K}]$ and $[\boldsymbol{M}]$ embody the elastic and mass properties of the metallic electrodes, respectively. There is no externally applied force at every node in the electrode finite-element mesh, except at the electrode/substrate boundary. Thus, it is possible to express the traction forces at the electrode/substrate interface, $\boldsymbol{f}_I$, in terms of the nodal displacements at the interface, $\boldsymbol{u}_I$, by:

$$\boldsymbol{f}_I = [\boldsymbol{Z}_S]\, \boldsymbol{u}_I, \tag{11}$$

where $[\boldsymbol{Z_S}]$ is the matrix that relates all nodal interface traction forces to the respective SH particle displacements at the electrode/substrate interface due to mass loading. The determination of surface stress from these traction forces is discussed in the next section, in which the FEM and BEM techniques are combined.

E. Combining Finite- and Boundary-Element Methods

The surface stress vector is defined by $\boldsymbol{T} = \left[T_4^{(1)}\ T_4^{(2)}\ \ldots\ T_4^{(N)}\right]^T$, where $T_4^{(n)}$ is the complex coefficient of the rectangular stress pulse on the n^{th} boundary element, and N is the total number of boundary elements for the entire IDT structure. The particle displacement within each finite element is interpolated linearly, and from Hooke's Law, the stress within the isotropic element is $T_4 = c_{44}\left(\partial u_2/\partial z\right)$ and is considered constant throughout each element. Thus, it is appropriate that the stress on the boundary elements be approximated using rectangular pulses. Likewise, the surface charge density is approximated using rectangular pulses and is represented by the charge density vector, $\boldsymbol{\sigma} = \left[\sigma^{(1)}\ \sigma^{(2)}\ \ldots\ \sigma^{(N)}\right]^T$ such that $\sigma^{(n)}$ is the charge density on the n^{th} boundary element.

The surface displacement vector $\boldsymbol{u} = \left[u_2(\Delta x)\ u_2(2\Delta x)\ \ldots\ u_2(N\Delta x)\right]^T$ comprises the particle displacements at the centers of the boundary elements. The displacement at each node at the interface is equal to the mean of the displacements found at the centers of the two adjacent boundary elements. Thus, $\boldsymbol{u}_I$ is linearly interpolated from $\boldsymbol{u}$ by $\boldsymbol{u}_I = [\boldsymbol{C}]\boldsymbol{u}$, where the matrix $[\boldsymbol{C}]$ performs this averaging, and from (11) the nodal traction forces at the interface are related to $\boldsymbol{u}$ by $\boldsymbol{f}_I = [\boldsymbol{Z}_S]\,[\boldsymbol{C}]\boldsymbol{u}$. The nodal forces at the endpoints of each element are averaged, and the result is divided by the element width and the unit aperture

to find $T_4^{(n)}$ [10]. Performing this operation on $[\boldsymbol{Z}_S]$ results in the matrix $[\boldsymbol{Z}_{TS}]$ which relates element stress to nodal displacements:

$$\boldsymbol{T} = [\boldsymbol{Z}_{TS}]\,[\boldsymbol{C}]\boldsymbol{u}. \tag{12}$$

Using (8), (9), and (12) one now can describe the relationship between surface charge density and potential, including the source effect of mass loading. The derivation is presented in Appendix A. The electrical potential on the boundary elements is represented by the potential vector $\boldsymbol{\phi} = \left[\phi^{(1)}\ \phi^{(2)}\ \ldots\ \phi^{(N)}\right]^T$ where $\phi^{(n)}$ is the voltage on the n^{th} boundary element. The convolution matrix $[\boldsymbol{H}]$, derived in Appendix A and given by (A24), relates surface potential to surface charge density, including the effect of mass loading.

The electrical admittance of the IDT for any arbitrary arrangement of electrode potentials is calculated by applying the following electrical boundary conditions: charge density for boundary elements located in the gaps between the electrodes is equal to zero, $\sigma_{gap} = 0$; the potential for boundary elements located on positive and negative electrodes, ϕ_{pos} and ϕ_{neg}, are $+V/2$ and $-V/2$, respectively, where V is the peak-to-peak applied voltage between electrodes; zero net charge on the transducer, $\sum_{n=1}^{N} \sigma^{(n)} = 0$. The unknown quantities are potential on the gap elements, ϕ_{gap}, and charge density on the electrode elements, σ_{elec}, which are found by way of constrained least-squares minimization. The total IDT current, I_{IDT}, is given by:

$$I_{IDT} = j\omega \Delta x W \sum_{m=1}^{M} \sigma_{pos}^{(m)} \tag{13}$$

where $\sigma_{pos}^{(m)}$ is the m^{th} complex charge density coefficient taken only on positive voltage electrodes; W is the IDT aperture; and M is the total number of boundary elements associated with positive electrodes. The electrical admittance is found by Ohm's Law, $Y(\omega) = I_{IDT}/V$.

F. Power Partitioning

The total power transduced by the IDT, $P_{TOT,IDT}$, may be divided into SH-SAW and SH-BAW contributions, as $P_{TOT,IDT} = P_{SH-SAW} + P_{SH-BAW}$. Partitioning electrical input power between SH-SAW and SH-BAW waves is performed using both numerical and analytical means as presented in [6] and [10]. At each frequency of interest, the Fourier transform of the surface stress and charge density distributions are computed for discrete values of k_x in order to determine the normal-mode weighting vector in (3). The fields, and thus the power spectral density of the SH-BAW mode, (dP_{SH-BAW}/dk_x), then may be calculated for all values of k_x. Because the SH-BAW exists over a finite interval of k_x, the total SH-BAW power radiated may be computed by numerical integration.

The power converted to SH-SAW is calculated using residue theory and is given by [6]:

$$P_{SH-SAW} = -\pi^2 \omega W \text{Re}\left(G_s \sigma\left(\omega s_o\right) \sigma\left(\omega s_o\right)^*\right), \tag{14}$$

where G_s is a coefficient used to approximate the simple poles in the electrostatic Green's function $\Gamma_{\phi\sigma}\left(s_x\right)$ used in (10). These poles are located at the free-surface SH-SAW slowness, $\pm s_o$, and are approximated as [6]:

$$\Gamma_{\phi\sigma(\text{pole})}\left(s_x\right) = \frac{G_s}{s_x - s_o} + \frac{-G_s}{s_x + s_o}. \tag{15}$$

III. Numerical and Experimental Results

A. Equipment Used

The numerical simulations reported in this work were performed using MATLAB™ Release 14 (The Mathworks, Inc., Natick, MA) on a Dell™ 530 Precision Workstation (Dell Inc., Round Rock, TX) operating Windows® XP Professional (Microsoft Inc., Redmond, WA). The system was configured with dual Intel Pentium 4 Xeon™ (Intel Inc., Santa Clara, CA) processors operating at 2.4 GHz and 4 Gb of system memory. The impedance measurements presented used an Agilent© 8753ES S-Parameter Network Analyzer (Agilent Technologies Inc., Palo Alto, CA) and a vibration isolated Cascade™ Microtech probe station (Cascade Microtech Inc., Beaverton, OR) with 150 μm pitch ground-signal-ground test probes. The IDT electrode thickness was measured using a Tencor Alphastep 500 surface profilometer (KLA Tencor, San Jose, CA).

B. Radiation Plots and Power Partitioning on Langasite

There are BAW propagation directions in certain anisotropic crystals for which the $\boldsymbol{k}$-vector may be oriented out of the substrate surface, whereas the power is still radiated to the bulk of the crystal. Fig. 2 shows the slowness surface of the SH-BAW in the sagittal plane of LGS (0°, 22°, 90°). The LGS constants used throughout this section have been taken from [20]. The bold portion of the curve indicates orientations for which the outward normal of the slowness curve has a $-z$ directed component. Eigenvectors corresponding to bulk waves radiated along these directions must be considered in the IDT power radiation analysis because they carry power away from the surface into the bulk of the crystal.

The distribution of bulk wave power with respect to the direction of propagation is given by [6]:

$$\frac{dP_{SH-BAW}}{d\theta_k} = \frac{dP_{SH-BAW}}{dk_x}\frac{dk_x}{d\theta_k}, \tag{16}$$

where $\theta_k = \tan^{-1}(k_z/kx)$ is the $\boldsymbol{k}$-vector direction with k_x and k_z as defined in (4). Fig. 3 plots the normalized BAW power distribution, $(dP_{SH-BAW}/d\theta_k)/P_{SH-BAW}$, as a function of the wave vector direction for a split-finger IDT along LGS (0°, 22°, 90°), $N_e = 78$ IDT electrodes with no guard electrodes, $\lambda = 32$ μm, mark-to-space ratio 1:1, and a uniform aperture $W = 50\lambda$. The region external to the IDT is completely metalized with an infinitesimally

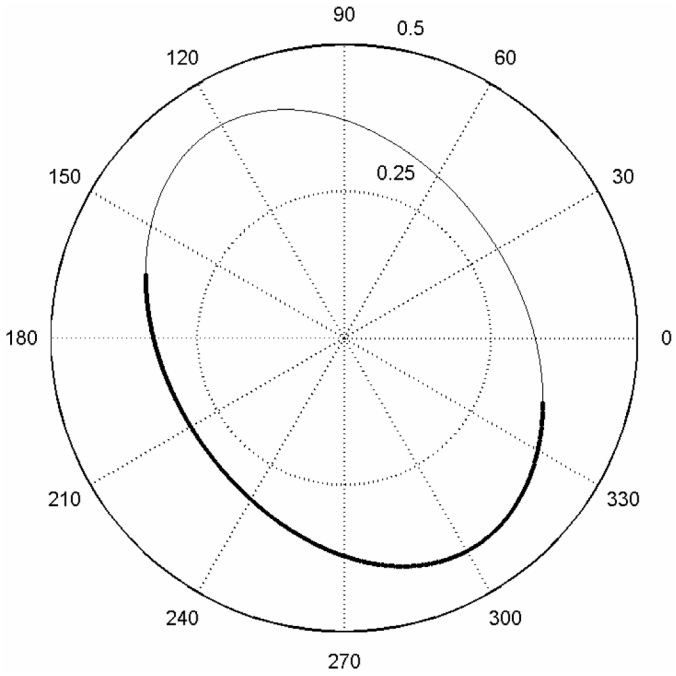

Fig. 2. SH-BAW slowness surface [s/km] in the sagittal plane of langasite, Euler angles (0°, 22°, 90°).

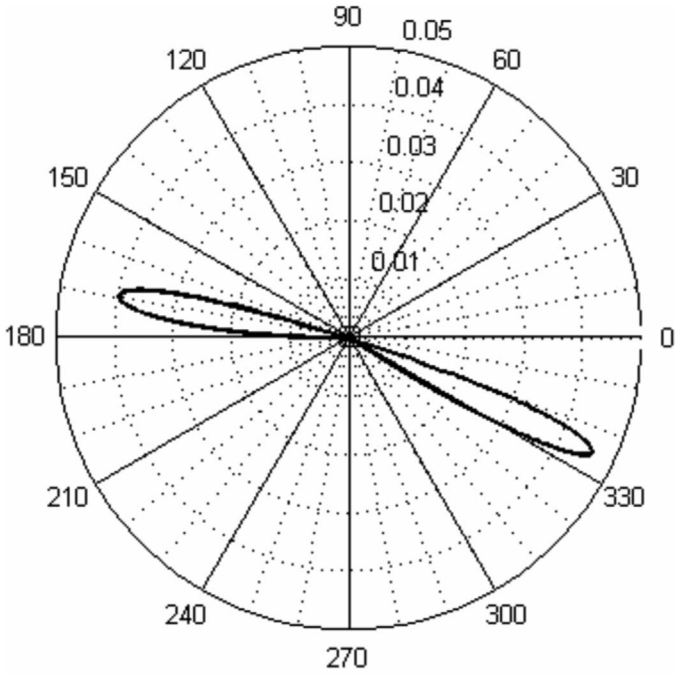

Fig. 3. SH-BAW power distribution normalized to total SH-BAW power, $(dP_{SH-BAW}/d\theta_k)/P_{SH-BAW}$, [1/degree], with respect to k-vector direction in LGS (0°, 22°, 90°), calculated at maximum conductance frequency, 93.121 MHz; split-finger IDT, $N_e = 78$, $\lambda = 32$ μm, $W = 50\lambda$, $a = 4$ μm, metalized case, ($P_{SH-BAW} = 0.303$ mW; $P_{TOT,IDT} = 0.481$ mW).

thin conducting film. Figs. 2 and 3 are very important in determining the crystal anisotropy, identifying the limits of integration in the calculation of total P_{SH-BAW}, and identifying which BAW modes and respective slowness values that contribute to the P_{SH-BAW} irradiated.

The crystal anisotropy that can be observed from Figs. 2 and 3 does not allow a proper visualization of the SH-BAW power radiation with depth. The SH-BAW radiation pattern inside the substrate [10] is given by:

$$\frac{dP_{SH-BAW}}{d\theta_A} = \frac{dP_{SH-BAW}}{dk_x}\frac{dk_x}{d\theta_A}, \tag{17}$$

where $\theta_A = \tan^{-1}(S_{z,SH-BAW}/S_{x,SH-BAW})$ is the radiation angle with respect to the surface of the substrate, and $S_{x,SH-BAW}$ and $S_{z,SH-BAW}$ are the x- and z-directed components of the Poynting vector of the SH-BAW traveling with the $\boldsymbol{k}$-vector direction θ_k. Fig. 4 plots the normalized BAW power radiation pattern $(dP_{SH-BAW}/d\theta_A)/P_{SH-BAW}$ with respect to radiation angle for the IDT referred to in Fig. 3.

The metalized boundary condition has three major effects in the SH-BAW behavior. The first effect under the metalized substrate condition the SH-BAW tilts into the substrate at a higher angle, with the peak of the main lobe going from 1.9 degrees in the case of free substrate to 6.3 degrees in the case of metalized substrate. The second effect refers to the reduction of the IDT power converted into SH-BAW, thus increasing the IDT power converted to SH-SAW. In fact, the BEM analysis shows that, for the metalized substrate case described by the IDT structure of Figs. 3 and 4, 37% of total IDT power is converted into SH-SAW, but in the case of free substrate only 0.96% of the total IDT power is converted to SH-SAW. The calculations performed in this work along LGS (0°, 22°, 90°) verified that, for the nonmetalized substrate case, more than 99% of the input power is delivered to the SH-BAW regardless of frequency, transducer length, or electrode thickness and metal type, a similar result to that obtained for PZT-4 in [6], and verified by the numerical routines developed in this work. The third effect of the metallization outside the IDT is an increase of the asymmetry of the SH-BAW main lobes, an effect that results from the crystal asymmetry that can be observed from Fig. 2.

Fig. 5 shows the percentage of IDT power converted to SH-SAW as a function of the number of IDT electrodes, N_e, when the LGS substrate surface outside the IDT structure is metalized. All of the simulated IDTs were split-electrode type, with 4 μm electrode width and mark-to-space ratio 1:1. The ratio P_{SH-SAW}/P_{IDT} was calculated at the frequency at which the peak SH-SAW conductance occurred. The four mass-loading cases considered are: Case 1, massless electrodes; Case 2, 2000 Å aluminum (Al) electrodes; Case 3, 1000 Å gold (Au) electrodes; Case 4, 2000 Å Au electrodes. The material constants for the Al and Au electrode layers used throughout this work have been taken from [21].

As can be noticed from Fig. 5, the effect of mass loading due to the finite IDT electrode mass must be considered in the IDT analysis, due to the modest SH-SAW piezoelectric coupling effect of the LGS orientation considered when compared to PZT-4 used in [6]. Fig. 5 shows that

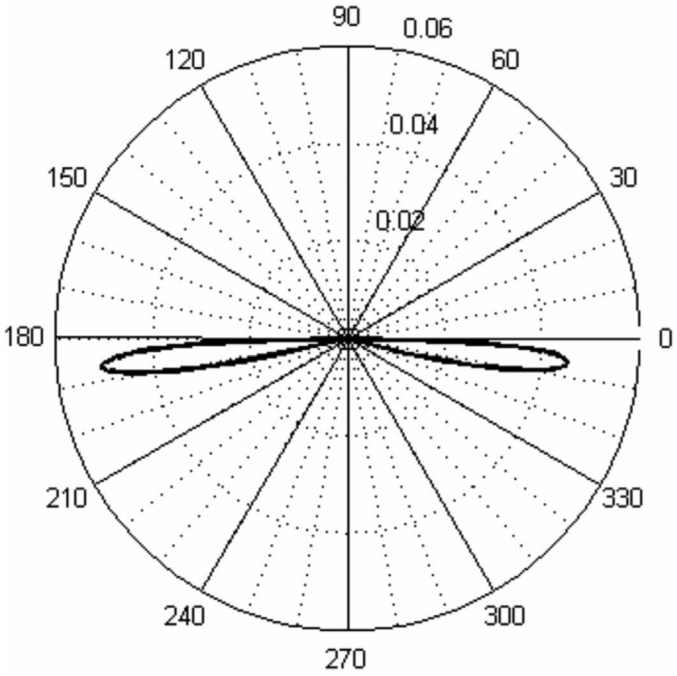

Fig. 4. SH-BAW power radiation pattern, normalized to total SH-BAW power, with respect to angle into the substrate, $(dP_{SH-BAW}/d\theta_A)/P_{SH-BAW}$ [1/degree] in LGS (0°, 22°, 90°), calculated at maximum conductance frequency, 93.121 MHz; split-finger IDT, $N_e = 78$, $\lambda = 32$ μm, $W = 50\lambda$, $a = 4$ μm, metalized case, ($P_{SH-BAW} = 0.303$ mW; $P_{TOT,IDT} = 0.481$ mW).

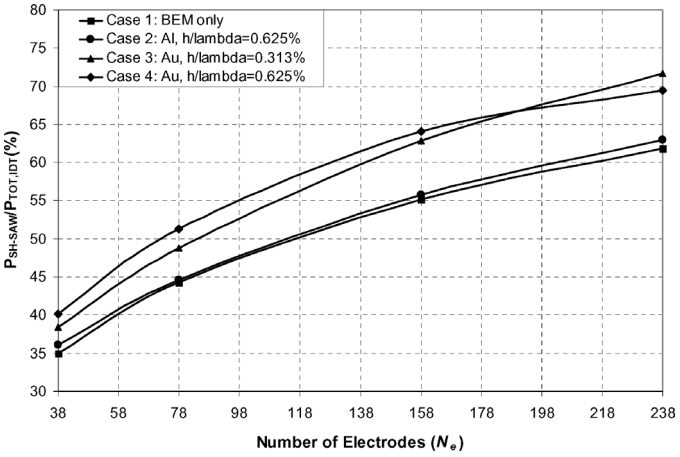

Fig. 5. Portion of input power delivered to SH-SAW versus number of electrodes, N_e, for LGS (0°, 22°, 90°); calculated at maximum SH-SAW conductance frequency; split-electrode IDT, $\lambda = 32$ μm, $W = 50\lambda$, $a = 4$ μm, metalized case.

for Au electrodes of thickness $h/\lambda = 0.00625$ the ratio $P_{SH-SAW}/P_{TOT,IDT}$ increased based on type of electrode material and thickness from 35% to 38.5% for $N_e = 38$; and from 44.4% to 48.8% for $N_e = 78$; and from 55.2% to 62.9% for $N_e = 158$; from 61.8% to 71.7% for $N_e = 238$. These results show that the metallic electrode film material and thickness can be used to increase the SH-SAW transduction efficiency, thus resulting in improved performance, less device insertion loss, and higher sensitivity in the case of a SH-SAW sensor.

C. Measured and Calculated IDT Admittance for the SH-SAW on Langasite

The FEM/BEM calculations and the measured devices reported in this section refer to the LGS propagation direction Euler angles (0°, 22°, 90°). The SH-SAW devices have been fabricated and tested at the University of Maine cleanroom and acoustic microwave laboratory facilities. The first transducer consists of a split-finger IDT fabricated on LGS (0°, 22°, 90°) with $N_e = 80$, finger width, $a = 4$ μm, uniform $W = 50\lambda$, and a mark-to-space ratio of 1:1. Six dummy electrodes were patterned on each side, and the regions outside of the IDT were mechanically and electrically free. The electrodes were composed of 1820 Å of radio frequency (RF) magnetron sputtered aluminum on top of 100 Å electron beam (e-beam) evaporated chromium (Cr) adhesion layer. Fig. 6 shows both calculated and measured electrical admittance responses for this device. During all simulations considered here, Δx did not exceed 2.1% of the SH-SAW wavelength, and the ratio of finite-element width to height did not exceed 8:1. Based on the numerical predictions discussed in the previous section, 99.1% of the IDT input power is delivered to the SH-BAW for this combination of IDT structure and LGS propagation direction. As can be observed from Fig. 6, the percent difference between the FEM/BEM simulated magnitude of the IDT admittance and the measurement is better than 5%.

In order to verify the FEM/BEM model when a more significant fraction of the total IDT power is converted to SH-SAW, devices have been fabricated in which the regions outside the IDT have been metalized. Two IDT structures have been fabricated and tested. The first one consists of a split-finger IDT fabricated on LGS (0°, 22°, 90°) with $N_e = 80$, finger width, $a = 4$ μm, uniform $W = 25\lambda$, and a mark-to-space ratio of 1:1. For this first IDT structure, a 720 Å Al film has been RF magnetron sputter deposited on top of a 100 Å e-beam evaporated Cr adhesion layer. For the second IDT structure, the same IDT dimensions have been used, but Au electrodes were sputter deposited to a thickness of 526 Å over 100 Å e-beam evaporated Cr adhesion layer. Figs. 7 and 8 compare calculated and measured results for these cases. The agreement between calculated and measured results is better in the case of Fig. 7, in which the Al film has been sputtered all over the device, when compared to Fig. 8, in which a heavier Au film has been sputtered all over the device, indicating that the thickness and material of the film outside the IDT (not considered in the calculations) significantly affects the IDT impedance.

The results in this section show that the FEM/BEM model implemented predicts IDT admittance to within 5% of measured values along LGS symmetry Type 4 orientations, including the effect of different types of IDT electrode metallization and thickness.

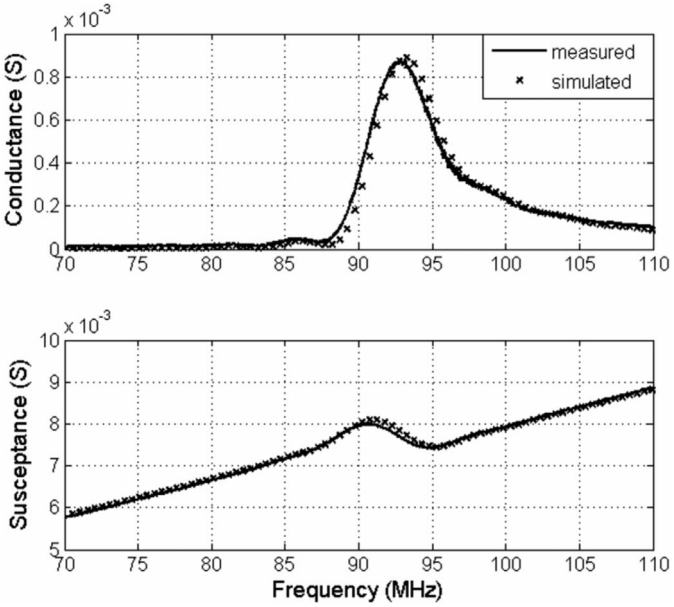

Fig. 6. Calculated and measured IDT admittance on LGS (0°, 22°, 90°); split-finger IDT, 1820 Å Al, 100 Å Cr, $N_e = 80$, $\lambda = 32$ μm, $W = 50\lambda$, $a = 4$ μm, nonmetalized case.

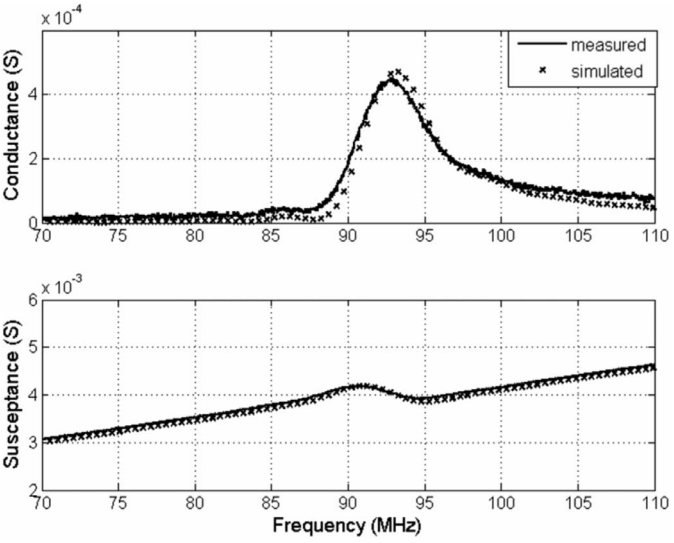

Fig. 7. Calculated and measured IDT admittance on LGS (0°, 22°, 90°); split-finger IDT, 720 Å Al, 100 Å Cr, $N_e = 80$, $\lambda = 32$ μm, $W = 25\lambda$, $a = 4$ μm, metalized case.

IV. Conclusions

The combined FEM/BEM IDT model implemented in this work has been used to calculate the IDT impedance considering both SH-SAW and SH-BAW piezoelectric active modes along the SH-cut LGS, Euler angles (0°, 22°, 90°), and the results have been compared to measured IDT impedances.

The effect of finite-thickness Al or Au electrodes and the presence (metalized case) or absence (nonmetalized case) of an infinitesimally thin metal guiding layer outside the IDT region have been included in the analysis.

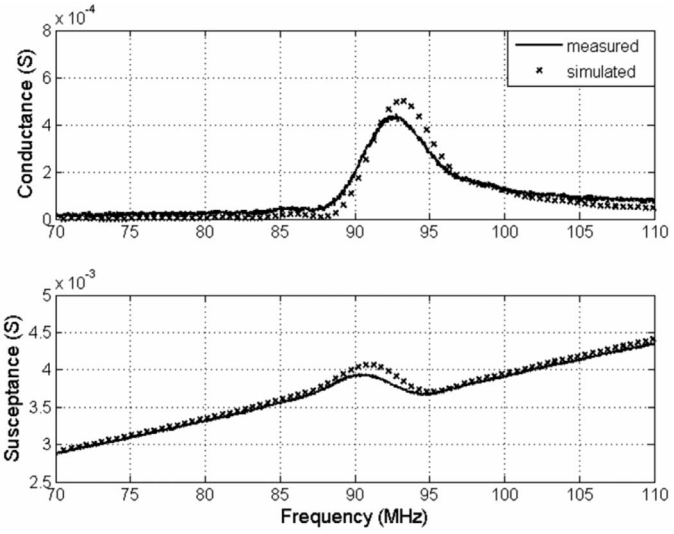

Fig. 8. Calculated and measured IDT admittance on LGS (0°, 22°, 90°); split-finger IDT, 526 Å Au, 100 Å Cr, $N_e = 80$, $\lambda = 32$ μm, $W = 25\lambda$, $a = 4$ μm, metalized case.

Around the device's operating frequency, the percent difference between calculated and measured magnitudes of the IDT impedance is better than 5%, considering the effect of mass loading by Al and Au IDT electrodes and both the metalized and nonmetalized cases.

Calculations of the IDT input power distribution between SH-SAW and SH-BAW, and therefore the calculation of the SH-SAW transduction efficiency, as a function of film type, thickness, and presence or absence of guiding films have been performed. It has been numerically verified that, for the nonmetalized case, less than 1% of IDT input power is converted to the SH-SAW mode, regardless of frequency, transducer length, and electrode thickness and metal type. That number increases to nearly 72% when a $N_e = 238$ split-electrode IDT, $h/\lambda = 0.63\%$ Au electrodes surrounded by an infinitesimally thin conducting film is used, a 9.9% improvement over aluminum electrodes of comparable thickness. This increase of nearly 10% in SH-SAW transduction efficiency, which can be achieved when heavier Au electrodes are used, directly reflects in lower device losses, improved SH-SAW based sensor sensitivity, and increase in the signal-to-noise ratio of the sensor.

Appendix A

The surface charge density was represented by the charge density vector $\boldsymbol{\sigma} = \left[\sigma^{(1)}\ \sigma^{(2)}\ \ldots\ \sigma^{(N)}\right]^T$, where $\sigma^{(n)}$ is the surface charge density on the n^{th} boundary element, and N is the total number of boundary elements. The actual surface charge density, $\sigma(x)$ may be expressed as a continuous function of position in terms of $\boldsymbol{\sigma}$ by:

$$\sigma(x) = \boldsymbol{cvect}(x) \cdot \boldsymbol{\sigma}, \tag{A1}$$

where:

$$\boldsymbol{cvect}(x) = \left[\text{rect}\left(\frac{x-\Delta x}{\Delta x}\right)\text{rect}\left(\frac{x-2\Delta x}{\Delta x}\right)\cdots\text{rect}\left(\frac{x-N\Delta x}{\Delta x}\right)\right]^T, \tag{A2}$$

and:

$$\text{rect}\left(\frac{x-m\Delta x}{\Delta x}\right) = \begin{cases} 1 \Rightarrow -\dfrac{\Delta x}{2} \le x - m\Delta x \le \dfrac{\Delta x}{2} \\ 0 \Rightarrow \text{otherwise} \end{cases}. \tag{A3}$$

For any position x, located on the m^{th} boundary element, the m^{th} element of $\boldsymbol{cvect}(x)$ is equal to 1, and the remaining elements are 0. Thus, at any location on the m^{th} boundary element, (A1) gives $\sigma(x) = \sigma^{(m)}$. Similarly, the T_4 surface stress component may be expressed in terms of $\boldsymbol{T}$ by:

$$T_4(x) = \boldsymbol{cvect}(x)\cdot\boldsymbol{T}. \tag{A4}$$

The forward and inverse Fourier transforms adopted in this work are defined, respectively, as:

$$\bar{f}(k_x) = \frac{1}{2\pi}\int_{-\infty}^{\infty} f(x)e^{jk_x x}dx, \tag{A5}$$

$$f(x) = \int_{-\infty}^{\infty} \bar{f}(k_x)\, e^{-jk_x x}dk_x. \tag{A6}$$

Applying the Fourier transform (A5) to $\boldsymbol{cvect}(x)$ gives:

$$\boldsymbol{cvect}(k_x) = \frac{\Delta x}{2\pi}\text{sinc}\left(k_x\frac{\Delta x}{2}\right)\boldsymbol{cvect}(x)\cdot \left[e^{jk_x\Delta x}\ e^{jk_x 2\Delta x}\ \cdots\ e^{jk_x N\Delta x}\right]. \tag{A7}$$

Because $\boldsymbol{T}$ and $\boldsymbol{\sigma}$ are independent of position, the Fourier transform of charge and surface stress, respectively, are given by:

$$\overline{\sigma}(k_x, z=0) = \boldsymbol{cvect}(k_x)\cdot\boldsymbol{\sigma}, \tag{A8}$$

$$\overline{T}_4(k_x, z=0) = \boldsymbol{cvect}(k_x)\cdot\boldsymbol{T}. \tag{A9}$$

where the overbar denotes that the quantity is given in the spectral domain, as indicated by (A5).

Combining (8), (9), (A8), and (A9), one obtains expressions for the particle displacement and surface potential in terms of $\boldsymbol{T}$ and $\boldsymbol{\sigma}$:

$$u_2(k_x) = \frac{\Gamma_{uT}}{\omega}\boldsymbol{cvect}(k_x)\cdot\boldsymbol{T} + \frac{\Gamma_{u\sigma}}{\omega}\boldsymbol{cvect}(k_x)\cdot\boldsymbol{\sigma}, \tag{A10}$$

$$\phi(k_x) = \frac{\Gamma_{\phi T}}{\omega}\boldsymbol{cvect}(k_x)\cdot\boldsymbol{T} + \frac{\Gamma_{\phi\sigma}}{\omega}\boldsymbol{cvect}(k_x)\cdot\boldsymbol{\sigma}. \tag{A11}$$

Applying the inverse transform given by (A6) to equation (A10), one obtains an integral expression for the real-space particle displacement:

$$u_2(x) = \int_{-\infty}^{\infty}\Big(\Gamma_{uT}\boldsymbol{cvect}(\omega s_x)\cdot\boldsymbol{T} + \Gamma_{u\sigma}\boldsymbol{cvect}(\omega s_x)\cdot\boldsymbol{\sigma}\Big)e^{-j\omega s_x x}ds_x. \tag{A12}$$

The particle displacement at the center on the m^{th} boundary element is equal to the mean displacement on the element, which is computed by applying:

$$u^{(m)} = \frac{1}{\Delta x}\int_{-\infty}^{\infty} u_2(x)\text{rect}\left(\frac{x-m\Delta x}{\Delta x}\right)dx. \tag{A13}$$

Inserting (A12) into (A13) results in an expression relating the displacement vector $\boldsymbol{u}$ to $\boldsymbol{T}$ and $\boldsymbol{\sigma}$:

$$\boldsymbol{u} = [\boldsymbol{\Phi}]\boldsymbol{T} = [\boldsymbol{\Lambda}]\boldsymbol{\sigma}. \tag{A14}$$

Combining (9), which relates the surface stress vector $\boldsymbol{T}$ to $\boldsymbol{u}$, and (A14), one obtains (A15), which gives the displacement vector $\mathbf{u}$ in terms of charge density, including the effect of mass loading by the IDT electrodes:

$$\boldsymbol{u} = \{[\boldsymbol{I}] - [\boldsymbol{\Phi}][\boldsymbol{Z}_{TS}][\boldsymbol{C}]\}^{-1}[\boldsymbol{\Lambda}]\boldsymbol{\sigma}, \tag{A15}$$

where:

$$[\boldsymbol{I}] = \text{Identity matrix}, \tag{A16}$$

$$\Lambda_{nm} = \frac{\Delta x}{2\pi}\int_{-\infty}^{\infty}\Gamma_{u\sigma}(s_x)\,\text{sinc}^2(0.5\omega s_x\Delta x) \times\exp(-j\omega s_x(n-m)\Delta x)ds_x, \tag{A17}$$

$$\Phi_{nm} = \frac{\Delta x}{2\pi}\int_{-\infty}^{\infty}\Gamma_{uT}(s_x)\,\text{sinc}^2(0.5\omega s_x\Delta x) \times\exp(-j\omega s_x(n-m)\Delta x)ds_x. \tag{A18}$$

Applying the inverse transform to (A11), one obtains an integral expression for the real-space surface potential, $\phi(x)$, given by:

$$\phi(x) = \int_{-\infty}^{\infty}\Big(\Gamma_{\phi T}\boldsymbol{cvect}(\omega s_x)\cdot\boldsymbol{T} + \Gamma_{\phi\sigma}\boldsymbol{cvect}(\omega s_x)\cdot\boldsymbol{\sigma}\Big)e^{-j\omega s_x x}ds_x. \tag{A19}$$

The potential is assumed uniform across each boundary element, and the potential on the m^{th} boundary element is given by:

$$\phi^{(m)} = \frac{1}{\Delta x}\int_{-\infty}^{\infty}\phi(x)\text{rect}\left(\frac{x-m\Delta x}{\Delta x}\right)dx. \tag{A20}$$

The surface potential vector is given by:

$$\boldsymbol{\phi} = [\boldsymbol{\Theta}]\boldsymbol{T} + [\boldsymbol{\Psi}]\boldsymbol{\sigma} \tag{A21}$$

where:

$$\Theta_{nm} = \frac{\Delta x}{2\pi}\int_{-\infty}^{\infty} \Gamma_{\phi T}(s_x)\,\mathrm{sinc}^2(0.5\omega s_x \Delta x) \times \exp(-j\omega s_x (n-m)\Delta x) ds_x, \tag{A22}$$

$$\Psi_{nm} = \frac{\Delta x}{2\pi}\int_{-\infty}^{\infty} \Gamma_{\phi\sigma}(s_x)\,\mathrm{sinc}^2(0.5\omega s_x \Delta x) \times \exp(-j\omega s_x (n-m)\Delta x) ds_x. \tag{A23}$$

Inserting (12) into (A21), and substituting (A15) for the displacement vector, one obtains (A24), in which the $\mathrm{N}\times\mathrm{N}$ convolution matrix $[\boldsymbol{H}]$ gives the potential vector $\boldsymbol{\phi}$ resulting from distributed surface charge $\boldsymbol{\sigma}$, including the source effect of mass loading:

$$\begin{aligned}\boldsymbol{\phi} &= [\boldsymbol{H}]\boldsymbol{\sigma} \\ &= \left([\boldsymbol{\Theta}][\boldsymbol{Z}_{TS}][\boldsymbol{C}]\left\{[\boldsymbol{I}] - [\boldsymbol{\Phi}][\boldsymbol{Z}_{TS}][\boldsymbol{C}]\right\}^{-1}[\boldsymbol{\Lambda}] + [\boldsymbol{\Psi}]\right)\boldsymbol{\sigma}.\end{aligned} \tag{A24}$$

Thus, the potential on the m^{th} boundary element resulting from the charge distribution over the entire IDT is given by $\phi^{(m)} = \sum_{n=1}^{N} H_{mn}\sigma^{(n)}$.

When regions outside of the IDT are metalized by an infinitesimally thin conducting film, the source of waves is instead surface normal stress, T_4, and tangential electric field, E_1. The resulting fields [6] are then particle displacement, u_2, and integrated charge, defined as $Q(x) = \int_{-\infty}^{x}\sigma(x)dx$. Spectral domain Green's functions are calculated for the metalized case, and the remaining analysis is unchanged with respect to the non-metalized case.

References

[1] V. Plessky, J. Koskela, S. Lehtonen, and M. M. Salomaa, "Surface transverse waves on langasite," in *Proc. IEEE Ultrason. Symp.*, 1998, pp. 139–142.

[2] M. Pereira da Cunha and D. C. Malocha, "Pure shear horizontal SAW on langatate," in *Proc. IEEE Ultrason. Symp.*, 2000, pp. 231–234.

[3] M. Pereira da Cunha, D. C. Malocha, D. R. Puccio, J. Thiele, and T. B. Pollard, "LGX pure shear horizontal SAW for liquid sensor applications," *IEEE Sens. J.*, vol. 3, pp. 554–561, Oct. 2003.

[4] E. Berkenpas, S. Bitla, P. Millard, and M. Pereira da Cunha, "LGS shear horizontal SAW devices for biosensor applications," in *Proc. IEEE Ultrason. Symp.*, 2003, pp. 1404–1407.

[5] S. Kakio, M. Nozawa, and Y. Nakagawa, "Shear-horizontal-type surface acoustic wave on langasite with Au or Ta_2O_5 thin film," in *Proc. IEEE Ultrason. Symp.*, 2003, pp. 2122–2125.

[6] R. F. Milsom, N. H. C. Reilly, and M. Redwood, "Analysis of generation and detection of surface and bulk acoustic waves by interdigital transducers," *IEEE Trans. Sonics Ultrason.*, vol. SU-24, pp. 147–166, May 1977.

[7] K. Inagawa and M. Koshiba, "Equivalent networks for SAW interdigital transducers," *IEEE Trans. Ultrason., Ferroelect., Freq. Contr.*, vol. 41, pp. 402–411, May 1994.

[8] V. P. Plessky and T. Thorvaldson, "Periodic Green's functions analysis of SAW and leaky SAW propagation in a periodic system of electrodes on a piezoelectric crystal," *IEEE Trans. Ultrason., Ferroelect., Freq. Contr.*, vol. 42, pp. 280–293, Mar. 1995.

[9] P. Ventura, J. M. Hodé, and B. Lopes, "Rigorous analysis of finite SAW devices with arbitrary electrode geometries, application to the calculation of reflection and scattering parameters," in *Proc. IEEE Ultrason. Symp.*, 1995, pp. 257–262.

[10] K. J. Gamble and D. C. Malocha, "Simulation of short LSAW transducers including electrode mass loading and finite finger resistance," *IEEE Trans. Ultrason., Ferroelect., Freq. Contr.*, vol. 49, pp. 47–56, Jan. 2002.

[11] K. Hashimoto, "Excitation and propagation of shear-horizontal-type surface and bulk acoustic waves," *IEEE Trans. Ultrason., Ferroelect., Freq. Contr.*, vol. 48, pp. 1181–1188, Sep. 2001.

[12] A. R. Baghai-Wadji, F. Seifert, and K. Anemogiannis, "Rigorous analysis of STWs in non-periodic arrays including mechanical and electrical interactions," in *Proc. IEEE Ultrason. Symp.*, 1988, pp. 303–306.

[13] J. Koskela, V. P. Plessky, and M. Salomaa, "Theory of shear horizontal surface acoustic waves in finite synchronous resonators," *IEEE Trans. Ultrason., Ferroelect., Freq. Contr.*, vol. 47, pp. 1550–1560, Nov. 2000.

[14] G. W. Farnell and E. L. Adler, "Elastic wave propagation in thin layers," in *Physical Acoustics*. vol. 9, W. P. Mason and R. N. Thurston, Eds. New York: Academic, 1972, pp. 35–127.

[15] M. Pereira da Cunha, "Extended investigation on high velocity pseudo surface waves," *IEEE Trans. Ultrason., Ferroelect., Freq. Contr.*, vol. 45, pp. 604–613, May 1998.

[16] E. L. Adler, "SAW and pseudo-SAW properties using matrix methods," *IEEE Trans. Ultrason., Ferroelect., Freq. Contr.*, vol. 1, pp. 876–882, Nov. 1994.

[17] J. Koskela, "Modeling SAW devices including mass-loading effects," Ph.D. dissertation, Helsinki University of Technology, Helsinki, Finland, 1998.

[18] B. A. Auld, *Acoustic Fields and Waves in Solids*. vol. 1, New York: Wiley, 1990.

[19] D. S. Burnett, *Finite Element Analysis*. Reading, MA: Addison-Wesley, 1987.

[20] A. Bungo, C. Jian, K. Yamaguchi, Y. Sawada, S. Uda, and Y. P. Pisarevsky, "Analysis of surface acoustic wave properties of the rotated y-cut langasite substrate," *Jpn. J. Appl. Phys.*, vol. 38, pp. 3239–3243, May 1999.

[21] O. L. Anderson, "Determination and some uses of isotropic elastic constants of polycrystalline aggregates using single-crystal data," in *Physical Acoustics*. vol. 3, pt. B, New York: Academic, 1965, pp. 77–83.

Thomas D. Kenny (S'99) was born in Fayetteville, NC, on May 12, 1977. He received the B.S. degree in electrical engineering in 1999 from the University of Maine, Orono, ME. He received the M.S. degree in electrical and computer engineering in 2003 from Georgia Institute of Technology, Atlanta, GA. He is currently pursuing the Ph.D. degree in electrical engineering at the University of Maine and plans to graduate in the fall of 2006.

He worked as a research technician from September, 1996, to August, 1999, for Sensor Research and Development Corporation, Orono, ME. He was an engineering intern during the summer of 2002 at Motorola Labs, Tempe, Arizona. Currently, he works in the Microwave Acoustics Laboratory at the University of Maine, Orono, ME. His research interests include SAW interdigital transducer modeling and new materials.

Mr. Kenny is a member of Eta Kappa Nu and Tau Beta Pi honor societies. He received National Science Foundation Research Experience for Undergraduates (NSF-REU) assistantships in 1996, 1997, and 1998, and was a student paper finalist at the 2004 IEEE Joint UFFC Symposium and at the 2005 IEEE International Ultrasonics Symposium.

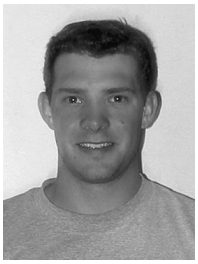

Thomas Bain Pollard (S'02) was born in Blue Hill, ME, on October 29, 1979. He received the B.S. degree in computer engineering at the University of Maine, Orono, ME, in 2003 and is currently pursuing his Ph.D. degree in the Department of Electrical and Computer Engineering at the University of Maine.

He has been involved with microwave acoustics research in the Microwave Acoustics Laboratory at the University of Maine's Laboratory for Surface Science and Technology (LASST) since the fall of 1999. As an undergraduate student he was a three time participant in the National Science Foundation Research Experience for Undergraduates (NSF-REU) summer program at the University of Maine. His current research interests are SAW liquid biosensors, new materials, shear horizontal SAW, and interdigital transducer modeling. He has twice been a student paper competition finalist at the 2003 and 2004 Utrasonics Symposia.

Eric Berkenpas (S'02) was born in Iowa in the United States in 1978. He received his B.S. degree in electrical engineering with a minor in computer science from the South Dakota State University in May of 2002. He received the M.S. degree in electrical engineering from the University of Maine, Orono, ME, in 2005. His research interests include surface acoustic wave devices, biological sensing, and sensor instrumentation.

Mauricio Pereira da Cunha (S'88–M'95–SM'02), born in Brazil in 1963, received the Bachelor's degree, 1985, and the Master's with Honors in electrical engineering, 1989, from the Escola Politécnica, Universidade de São Paulo. Master's thesis title is "Design and Implementation of a 70 MHz SAW Convolver." He received the Ph.D. degree, Dean's Honor List, from McGill University, Montreal, PQ, Canada, in electrical engineering in 1994. Ph.D. thesis title is "SAW Propagation and Device Modeling on Arbitrarily Oriented Substrates".

Mauricio has worked with the Microwave Devices R&D Group at NEC (Nippon Electric Co.), Brazil, Laboratório de Microeletrônica, Escola Politécnica, Department of Electrical Engineering, Universidade de São Paulo, McGill University, Montreal, PQ, Canada, and SAWTEK Inc., Orlando, FL. He passed a sabbatical year at University of Central Florida, Consortium for Applied Acoustoelectronic Technology (CAAT), Orlando, FL, where he worked in cooperation with Piezotechnology Inc, on the characterization of new piezoelectric materials, namely langatate, langanite, and langasite, and with bulk and surface acoustic wave devices. Mauricio was a Professor in the Department of Electronic Engineering, Universidade de São Paulo until he joined the Department of Electrical and Computer Engineering at the University of Maine in 2001.

Dr. Pereira da Cunha is a member of the IEEE, Sigma Xi, and of the Brazilian Microwave Society (SBMO). He was elected to serve on the SBMO Administrative Committee from 1996 to 1999. He is a reviewer for the IEEE UFFC TRANSACTIONS, and he has been a member of the IEEE International Ultrasonics Symposium Technical Program Committee since 1997. He has served on the UFFC-Society Administrative Committee from 2002–2004. At Ultrasonics Symposia he gave the invited paper,"High Velocity Pseudo Surface Acoustic Waves (HVPSAW): Further Insight," in 1996, and presented the short course, "SAW, PSAW, and BAW Materials and Devices" in 2000. He wrote the invited paper "Pseudo and High Velocity Pseudo SAWs," for the International Journal of High Speed Electronics and Systems (IJHSES), also published as a chapter in the book Advances in SAW Technology, Systems and Application, vol. 2, Singapore, (2001).